Toxicology 250 (2008) 15–26

Contents lists available at ScienceDirect

Toxicology

journal homepage: www.elsevier.com/locate/toxicol

A toxicogenomics approach for early assessment of potential non-genotoxic hepatocarcinogenicity of chemicals in rats

Takeki Uehara [a], Mitsuhiro Hirode [a], Atsushi Ono [a], Naoki Kiyosawa [a], Ko Omura [a], Toshinobu Shimizu [a], Yumiko Mizukawa [a,b], Toshikazu Miyagishima [a], Taku Nagao [a,c], Tetsuro Urushidani [a,b,*]

[a] Toxicogenomics Project, National Institute of Biomedical Innovation, 7-6-8 Asagi, Ibaraki, Osaka 567-0085, Japan
[b] Department of Pathophysiology, Faculty of Pharmaceutical Sciences, Doshisha Women's College of Liberal Arts, Kodo, Kyotanabe, Kyoto 610-0395, Japan
[c] National Institute of Health Sciences, 1-18-1 Kamiyoga, Setagaya-Ku, Tokyo 158-8501, Japan

ARTICLE INFO

Article history:
Received 14 March 2008
Received in revised form 15 May 2008
Accepted 20 May 2008
Available online 29 May 2008

Keywords:
Toxicogenomics
Rat
Liver
Hepatocarcinogenesis
Non-genotoxic

ABSTRACT

For assessing carcinogenicity in animals, it is difficult and costly, an alternative strategy has been desired. We explored the possibility of applying a toxicogenomics approach by using comprehensive gene expression data in rat liver treated with various compounds. As prototypic non-genotoxic hepatocarcinogens, thioacetamide (TAA) and methapyrilene (MP) were selected and 349 commonly changed genes were extracted by statistical analysis. Taking both compounds as positive with six compounds, acetaminophen, aspirin, phenylbutazone, rifampicin, alpha-naphthylisothiocyanate, and amiodarone as negative, prediction analysis of microarray (PAM) was performed. By training and 10-fold cross validation, a classifier containing 112 probe sets that gave an overall success rate of 95% was obtained. The validity of the present discriminator was checked for 30 chemicals. The PAM score showed characteristic time-dependent increases by treatment with several non-genotoxic hepatocarcinogens, including TAA, MP, coumarin, ethionine and WY-14643, while almost all of the non-carcinogenic samples were correctly predicted. Measurement of hepatic glutathione content suggested that MP and TAA cause glutathione depletion followed by a protective increase, but the protective response is exhausted during repeated administration. Therefore, the presently obtained PAM classifier could predict potential non-genotoxic hepatocarcinogenesis within 24 h after single dose and the inevitable pseudo-positives could be eliminated by checking data of repeated administrations up to 28 days. Tests for carcinogenicity using rats takes at least 2 years, while the present work suggests the possibility of lowering the time to 28 days with high precision, at least for a category of non-genotoxic hepatocarcinogens causing oxidative stress.

1. Introduction

Chemical carcinogenesis is a multistage process, *i.e.*, initiation, promotion and progression (Dragan et al., 1993; Miller and Miller, 1981; Scott et al., 1984). Based on this mechanism of action, chemical carcinogens are classified as genotoxic (mutagenic) and non-genotoxic (non-mutagenic) agents (Hayashi, 1992; Melnick et al., 1996). Genotoxic agents covalently react with DNA to form DNA adducts within the cells of the target organ, contributing to the initiation process. Such chemicals could be assessed by several short-term *in vitro* and *in vivo* assays that measure DNA damage, mutagenic effects, and chromosomal aberrations (Weisburger and Williams, 2000). In the case of non-genotoxic agents, the mechanism is much more complicated. Non-genotoxic carcinogens lack chemical reactivity with DNA and hence do not form DNA adducts, but rather induce effects that indirectly lead to neoplastic transformation or enhance the development of tumors from pre-initiated cells. Although the mechanism of action of such non-genotoxic carcinogens is not fully understood, several possibilities have been postulated in liver, such as oxidative stress, modulation of metabolizing enzymes, induction of peroxisome proliferation, alteration of intercellular communication, and disruption of the balance between proliferation and apoptosis (Butterworth and Bogdanffy, 1999; Cohen and Ellwein, 1990; Klaunig et al., 1998; Klaunig and Kamendulis, 2004; Nguyen-Ba and Vasseur, 1999; Silva Lima and Van der Laan, 2000; Williams et al., 1996). Even more complicated is the fact that many non-genotoxic carcinogens frequently cause several of these effects at once. The effects of non-genotoxic

* Corresponding author at: Department of Pathophysiology, Faculty of Pharmaceutical Sciences, Doshisha Women's College of Liberal Arts, Kodo, Kyotanabe, Kyoto 610-0395, Japan. Tel.: +81 72 641 9826; fax: +81 72 641 9850.
E-mail address: turushid@dwc.doshisha.ac.jp (T. Urushidani).

0300-483X/$ – see front matter © 2008 Elsevier Ireland Ltd. All rights reserved.
doi:10.1016/j.tox.2008.05.013

carcinogens in rodents are only manifested after *in vivo* exposure at high dosage levels over long periods (*e.g.*, 2-year rodent carcinogenicity assays). Consequently, the current strategy for evaluating non-genotoxic carcinogens is not satisfactory because the test is time consuming and expensive, and it requires the use of many animals and large amounts of chemicals.

The present report is focused on the application of toxicogenomics for early assessment of potential non-genotoxic hepatocarcinogenicity of chemicals. Non-genotoxic hepatocarcinogenesis has been studied extensively, and postulated to act via a number of mechanisms: oxidative stress, increased mitogenesis, decreased apoptosis, interference with gap junction intercellular communication, and interference with tubulin polymerization (Combes, 2000; Klaunig et al., 1998). Several recent publications have described applications of microarrays and expression profiling for non-genotoxic carcinogenesis in liver (Ellinger-Ziegelbauer et al., 2005, 2008; Fielden et al., 2007; Nie et al., 2006). They attempted to extract common gene sets coordinately deregulated by several different classes of genotoxic and/or non-genotoxic hepatocarcinogenesis. It was then revealed that the modulation of extracted genes was dependent upon the class of the carcinogenesis. This strongly suggests that mechanism-based strategy should be employed in order to obtain useful biomarker gene sets for carcinogenesis. The specific aim of the present study was to develop identifiers for early assessment of non-genotoxic hepatocarcinogenicity in specific class of chemical based on gene expression profiles in reference to our large-scale database named as TG-GATEs (genomics assisted toxicity evaluation system developed by Toxicogenomics Project, Japan) (Urushidani, 2007). Our strategy was to focus on common gene expression changes in livers treated with two well-known oxidative stressors, methapyrilene (MP) (Lijinsky et al., 1980; National Toxicology Program, 2000; Ohshima et al., 1984; Ratra et al., 1998) and thioacetamide (TAA) (Becker, 1983; Diez-Fernandez et al., 1998; Duivenvoorden and Maier, 1994; Ohtsuka et al., 1998; Sanz et al., 1995) to identify a characteristic set of genes reflecting the early stage of oxidative stress-mediated non-genotoxic hepatocarcinogenesis.

2. Materials and methods

2.1. Animals and experimental design

Five-week-old male Sprague–Dawley rats were obtained from Charles River Japan, Inc. (Kanagawa, Japan). After a 7-day quarantine and acclimatization period, the animals (6-week old) were assigned to dosage groups (five rats per group) using a computerized stratified random grouping method based on individual body weight. The animals were individually housed in stainless-steel cages in an animal room that was lighted for 12 h (7:00–19:00) daily, ventilated with an air-exchange rate of 15 times per hour, and maintained at 21–25 °C with a relative humidity of 40–70%. Each animal was allowed free access to water and pellet diet (CRF-1, sterilized by radiation, Oriental Yeast Co., Ltd., Tokyo, Japan).

Table 1 lists the overview of the compounds used in this study. A total of 30 compounds (10 non-genotoxic hepatocarcinogens and 20 non-hepatocarcinogens) were available in the database when the present analysis was performed. They were subdivided in a training set, consisting of 2 non-genotoxic carcinogens (positive training set) and 6 non-hepatocarcinogens (negative training set) with the test set for additional validation consisting of 8 non-genotoxic carcinogens and 14 non-hepatocarcinogens.

According to the standard protocol in our project (Takashima et al., 2006), five rats per group were orally administered at three doses with these compounds suspended or dissolved either in 0.5% methylcellulose (MC) solution or corn oil according to their dispersibility. Traditionally, carcinogenicity studies for chemical agents have relied upon the maximally tolerated dose (MTD) as the standard method for high dose selection. In the present study, the MTD was chosen based on data derived from preliminary toxicity studies of 7 days duration.

For single-dose studies, rats were sacrificed at 3, 6, 9 and 24 h after dosing (3H, 6H, 9H and 24H, respectively). For repeated dose studies, the animals were treated daily for 3, 7, 14 and 28 days, and sacrificed 24 h after the last dosing [day 4 (4D), 8 (8D), 15 (15D) and 29 (29D), respectively]. The animals were euthanized by exsanguination from the abdominal aorta under ether anesthesia, and the liver samples were obtained from the left lateral lobe of the liver in each animal immediately after sacrifice for examination.

The experimental protocols were reviewed and approved by the Ethics Review Committee for Animal Experimentation of National Institute of Health Sciences.

2.2. Histopathology of livers treated with MP or TAA

For light microscopical examination, the liver sample of each animal was fixed in 10% neutral buffered formalin, dehydrated in alcohol and embedded in paraffin. Paraffin sections were prepared and stained by a routine method with hematoxylin and eosin (H&E).

2.3. Microarray analysis

An aliquot of the sample (about 30 mg) for microarray analysis was obtained from the left lateral lobe of the liver in each animal immediately after sacrifice, kept in RNAlater® (Ambion, Austin, TX, USA) overnight at 4 °C, and then frozen at −80 °C until use. Liver samples were homogenized with the buffer RLT supplied in RNeasy Mini Kit (Qiagen, Valencia, CA, USA), and total RNA was isolated according to the manufacturer's instructions. Microarray analysis was conducted on three out of five samples for each group by using GeneChip® RAE230A probe arrays (Affymetrix, Santa Clara, CA, USA). The procedure was basically conducted according to the manufacture's instructions as previously reported (Uehara et al., 2008a,b). Microarray Analysis Suite 5.0 (MAS; Affymetrix) was used to quantify microarray signals and the intensities were normalized for each chip by setting the mean intensity to 500 (per chip normalization).

2.4. Selection of persistently up/down-regulated genes in common with MP and TAA

By using statistical and clustering tools, persistently up/down-regulated genes in common with MP and TAA throughout the study periods were extracted. First, data were imported into GeneSpring 6.0 software (Silicon Genetics, Redwood City, CA), and comparisons among time-matched groups from each study of MP and TAA were performed using one-way analysis of variance (ANOVA) with Tukey's multiple comparison test for post hoc comparisons when significance was determined by ANOVA with a false discovery rate ($p < 0.05$). Probe sets exhibiting significant changes in expression by Tukey's multiple comparison test in both high- and middle-dose groups for one or more time points in each study were selected. In the next step, significant selected probe sets (452 probe sets) were divided into subsets with distinct expression profiles by K-means clustering using Tigr Mev 3.1 software (http://www.tm4.org/mev.html) (current metric: Euclidean distance; divided into nine clusters) based on logarithm (log 2) of the ratio to control for individual gene expression. Genes not categorized in the clusters showing clear time- and dose-independent expression pattern were excluded from further analysis. Finally, a subset of 349 probe sets containing 276 up-regulated and 73 down-regulated probe sets was selected for common intersection to single and repeated studies of MP and TAA (for more information, see supplemental figures).

2.5. Class discrimination by prediction analysis of microarray (PAM)

Prediction of potential carcinogenesis was performed by an approach using PAM for R package (http://www-stat.stanford.edu/~tibs/PAM). PAM makes sample classification using the nearest shrunken centroid method with an automated gene selection step integrated into the algorithm (Tibshirani et al., 2002). It employs a parameter threshold Δ to select genes for class discrimination. PAM training is performed by comparing 2 positive compounds as non-genotoxic carcinogenesis (MP and TAA, high dose group only) with 6 negative compounds, *i.e.*, APAP (Iida et al., 2005; National Toxicology Program, 1993), ASA (Giri, 1993), PhB (Meakawa et al., 1987; National Toxicology Program, 1990), RIF (Sodhi et al., 1997), ANIT (Jean and Roth, 1995; Leonard et al., 1981) and AM (Agoston et al., 2003; Delaney et al., 2004) for the ratio of expression levels of the selected 349 probe sets at various time points (a total of 64 training samples).

Ten-fold cross validation was performed to find out the optimal classifier performance, which minimized classification errors for training sets. During the validation, a threshold Δ was varied in search of the optimal classifier performance. The Δ value that settled at the lowest classification error with the fewest genes was favored as the optimal. For validation of the classifier, the optimized threshold value obtained from training was subsequently used for prediction of potential carcinogenicity for the total of 30 compounds, including training sets. PAM prediction results were expressed as a logarithm transformed score (PAM prediction score) of the ratio of positive class probability relative to negative class probability associated with the classification of each sample, *i.e.*,

$$\text{PAM prediction score} = \log_{10} \frac{\text{class probability : positive}}{\text{class probability : negative}}$$

Table 1
Overview of the compounds used for prediction analysis of microarrays training and/or test

Compound	Abbreviation	CAS-number	Mode of action	Supplier	Vehicle	Dose (mg/kg)	PAM training/test
Non-genotoxic hepatocarcinogens[a,b]							
Methapyrilene	MP	135-23-9	Oxidative stress induction	Sigma	0.5%MC	10, 30, 100	Positive training/test set
Thioacetamide	TAA	62-55-5	Oxidative stress induction	Sigma	0.5%MC	4.5, 15, 45	Positive training/test set
Coumarin	CMA	91-64-5	Oxidative stress induction	Tokyo Chemical Industry	Corn oil	150	Test set
Ethionine	ET	67-21-0	Oxidative stress induction	Tokyo Chemical Industry	0.5%MC	250	Test set
Carbon tetrachloride	CCL4	56-23-5	Oxidative stress induction	Wako Pure Chemical Industries	Corn oil	300	Test set
Phenobarbital	PB	57-30-7	Hepatic enzyme induction	Sigma	0.5%MC	100	Test set
Hexachlorobenzene	HCB	118-74-1	Hepatic enzyme induction	Tokyo Chemical Industry	Corn oil	300	Test set
Clofibrate	CFB	637-07-0	Peroxisome proliferation	Wako Pure Chemical Industries	Corn oil	300	Test set
Gemfibrozil	GFZ	25812-30-0	Peroxisome proliferation	Sigma	Corn oil	300	Test set
Wy-14,643	WY	50892-23-4	Peroxisome proliferation	Tokyo Chemical Industry	Corn oil	100	Test set
Non-hepatocarcinogens[a,b]							
Acetaminophen	APAP	103-90-2	–	Sigma	0.5%MC	600	Negative training set
Aspirin	ASA	50-78-2	–	Wako Pure Chemical Industries	0.5%MC	450	Negative training set
Phenylbutazone	PhB	50-33-9	–	Sigma	0.5%MC	200	Negative training set
Rifampicin	RIF	13292-46-1	–	Wako Pure Chemical Industries	0.5%MC	200	Negative training set
Alpha-naphthylisothiocyanate	ANIT	551-06-4	–	Tokyo Chemical Industry	Corn oil	15	Negative training set
Amiodarone hydrochloride	AM	1951-25-3	–	Sigma	0.5%MC	200	Negative training set
Allopurinol	APL	315-30-0	–	Sigma	0.5%MC	150	Negative test set
Allyl alcohol	AA	107-18-6	–	Tokyo Chemical Industry	Corn oil	30	Negative test set
Benzbromarone	BBr	3562-84-3	–	Sigma	0.5%MC	200	Negative test set
Bromobenzene	BBZ	108-86-1	–	Tokyo Chemical Industry	Corn oil	300	Negative test set
Carbamazepine	CBZ	298-46-4	–	Sigma	0.5%MC	300	Negative test set
Chlorpromazine	CPZ	69-09-0	–	Wako Pure Chemical Industries	0.5%MC	45	Negative test set
Diclofenac sodium	DFNa	15307-79-6	–	Cayman Chemical Company	0.5%MC	10	Negative test set
Diazepam	DZP	439-14-5	–	Wako Pure Chemical Industries	0.5%MC	250	Negative test set
Isoniazid	INAH	54-85-3	–	Sigma	0.5%MC	200	Negative test set
Nitrofurantoin	NFT	67-20-9	–	ICN Biomedicals	0.5%MC	100	Negative test set
Phenytoin	PHE	57-41-0	–	Tokyo Chemical Industry	0.5%MC	600	Negative test set
Propylthiouracil	PTU	51-52-5	–	Tokyo Chemical Industry	0.5%MC	100	Negative test set
Sulfasalazine	SS	599-79-1	–	Sigma	0.5%MC	1000	Negative test set
Valproate sodium	VPA	1069-66-5	–	Sigma	0.5%MC	450	Negative test set

[a] Genotoxicity is based on *in vitro* genotoxicity tests (Salmonella and mammalian gene mutation tests) as reviewed in NTP (http://ntp-server.niehs.nih.gov/), IARC (http://monographs.iarc.fr.) and several published papers.

[b] Carcinogenicity is based on reviews by NTP (http://ntp-server.niehs.nih.gov/), IARC (http://monographs.iarc.fr.) and several published papers.

2.6. Gene ontology (GO) analysis of PAM classifier

The identified probe sets were subjected to GO analysis by DAVID (database for annotation, visualization, and integrated discovery; http://apps1.niaid.nih.gov/david/) using Fisher's exact test. Level 3 analysis was adopted.

2.7. Measurement for hepatic total glutathione contents

Hepatic total glutathione was measured in the liver of rats receiving a high dose of MP, TAA or BBZ, and their corresponding controls. Measurements were performed for three rats (gene expression was measured) per group using Glutathione Quantification Kit (Dojindo Mol. Tech, Inc., Kumamoto, Japan). In brief, the liver tissue was homogenized in 5% 5-sulfosalicylic acid and the particulate cellular debris was removed by centrifugation (8000 × g) for 10 min. The internal standards consist of serial dilutions of glutathione (1000, 750, 500, 250, 100, 50 and 0 μM). The change in absorbance at 405 nm was measured and total glutathione was calculated according to the glutathione standard curve. The results were analyzed with the use of an unpaired two-tailed Student's *t*-test or Welch's *t*-test as appropriate, and a *p*-value of <0.05 was considered statistically significant.

3. Results

3.1. Histopathology

Except for the death of one animal in the high dose group of MP on 20D, there were no other deaths in these studies of MP and TAA.

MP- or TAA-treated rats revealed typical liver damage throughout the study periods. Although the extent of the liver damage differed slightly among the animals, a similar pattern was obtained for those in the same dose group.

At high dosage of MP in the single dose study, periportal hepatocytes exhibited hypertrophy characterized by granular eosinophilic cytoplasm and enlarged nuclei with variable anisonucleosis at each time point. More striking abnormalities include mononuclear cell infiltration and hepatocellular single cell necrosis containing shrunken cells with pyknotic nuclei randomly scattered throughout the periportal region of the hepatic lobule. Associated with these lesions, increased numbers of hepatocellular mitotic figures and bile duct hyperplasia were present at each time point in the repeated dose study. At 29D, hepatocellular hyperplasia became evident, and some affected portal regions contained an increased number of oval cells arranged in clusters without a distinct lumen (Fig. 1a). In addition, for the same dose group, a pre-neoplastic altered hepatocellular focus was also observed (Fig. 1b). Middle-dose MP treatment resulted in minimal hepatocellular hypertrophy, single cell necrosis of hepatocytes, and mononuclear cell infiltration in the periportal region at 15D and 29D. Moreover, no significant histopathological alterations were observed at early time points except hepatocellular hypertrophy. In the low-dose MP-treated groups, no significant changes were observed throughout the study periods except for minimal hypertrophy of hepatocytes, observed in one animal each at 8D and 29D.

At high- and middle-dose of TAA, centrilobular hepatocytes exhibited hypertrophy with large, atypical nuclei in single and repeated dose studies (Fig. 1c). Moreover inflammatory cell infiltration and hepatocellular single cell necrosis were also observed at the centrilobular region. The degree of these lesions increased in a dose and time-dependent manner. At 15D and 29D, bile duct hyperplasia and oval cell proliferation at the periportal region became evident, and a pre-neoplastic altered hepatocellular focus was also observed (Fig. 1d). No significant histopathological alterations were observed in the low-dose groups throughout the study periods except degeneration of hepatocytes with granular and eosinophilic cytoplasm, observed in two animals at 29D.

3.2. Class discrimination by PAM in the training set

PAM training was performed using the training set to identify a minimal subset of genes expected to best characterize the early stage of non-genotoxic hepatocarcinogenesis-specific responses. Fig. 2 shows the training and cross-validation errors for different threshold values. Both the training and cross-validated errors were minimized near the threshold = 4.00, where 112 genes were selected. At this threshold, both classes of the training samples were clearly separated based on the expression pattern of these 112 genes with an overall success rate of 95%. Namely, 13 of the 16 positive sets (81%) and all of the negative sets (100%) were correctly classified (Fig. 3a). However, three positive sets (MP-3H, -4D and TAA-3H) were classified as negative, together with all of the negative sets (Fig. 3b).

The list of the genes involved in the PAM classifier is shown in Table 2 (for more information, see supplemental data). Genes were sorted according to the best prediction between the two classes. The top three important discriminators identified by PAM were "nuclear RNA helicase, DECD variant of DEAD box family (Ddx39)", "interferon-related developmental regulator 1 (Ifrd1)", and "mdm2, transformed mouse 3T3 cell double minute 2 (Mdm2)", which were highly up-regulated by MP and TAA. In the extracted 112 probe sets, 111 were prominently up-regulated in the positive training set and the remaining 1 gene (cytochrome P450 4F4) was down-regulated. Based on gene ontology, the contents of genes related to cellular metabolism including several anti-oxidative metabolism, cell proliferation, cell cycle, response to DNA damage stimulus were significantly high (Table 3). These features might reflect the cellular changes related to sustained oxidative stress in association with non-genotoxic hepatocarcinogenesis by MP and TAA.

3.3. Validation of usefulness of the PAM classifier

The 112-gene classifier generated on the training set was next applied to class discrimination for the 30 total compounds as a validation test. The classifier predicted the following samples as positive: high dose MP-6H, 9H, 24H, 8D, 15D and 29D; middle-dose TAA-29D; high dose TAA-6H, 9H, 24H, 4D, 8D, 15D and 29D; CMA-3H, 6H and 9H; ET-24H, 4D, 8D, 15D and 29D; WY-15D and 29D; BBZ-24H. All of other samples (including enzyme inducers, PB and HCB; peroxisome proliferators other than WY, such as CFB and GFZ; and other compounds) were predicted as negative.

In the present study, these prediction results were visualized as a numerical score reflecting the probabilities of class discrimination between the two classes, namely the PAM prediction score. The PAM score showed characteristic time-dependent changes by treatment with several non-genotoxic hepatocarcinogens. In the MP- or TAA-treated group, the score increased dose-dependently with a peak value at 6H for MP, 9H and 24H for TAA after single dosing, and then it markedly increased with repeated administrations (Fig. 4b, c, e, f). CMA, ET or WY treatment also resulted in an increase in the score with a peak value at 6H for CMA, 24H for ET and WY, and also showed an increase or tendency to increase with repeated dosing (Fig. 4g, h, j). Although all of the CCL4-treated groups were predicted as negative, the score showed a tendency to increase with repeated dosing (Fig. 4i). On the other hand, all of the low dose MP- or TAA-treated groups were predicted as negative without any tendency to increase in the score with repeated dosing (Fig. 4a and d). As for the enzyme inducers with carcinogenic activity, PB and HCB (Fig. 4l and m), and peroxisome proliferators other than WY, i.e., CFB (Fig. 4n) and GFZ (within Fig. 4r), showed negative scores throughout the time points. Of the non-carcinogenic samples, BBZ showed a transient increase in the score at 24H but returned to negative during repeated dosing (Fig. 4k). Other non-carcinogenic

Table 2
The list of the genes involved in the PAM classifier

Probe ID	Accession number	Gene title	Gene symbol
1387048_at	NM_053563	DEAD (Asp-Glu-Ala-Asp) box polypeptide 39	Ddx39
1367795_at	NM_019242	Interferon-related developmental regulator 1	Ifrd1
1384427_at	XM_001080981	Transformed mouse 3T3 cell double minute 2 homolog (mouse) (predicted)	Mdm2_predicted
1388986_at	–	EST	–
1369921_at	NM_020540	Glutathione S-transferase M4	Gstm4
1368072_at	NM_019290	B-cell translocation gene 3	Btg3
1387060_at	NM_031642	Kruppel-like factor 6	Klf6
1376098_a_at	XM_001069724	Myosin IG	Myo1g
1368173_at	NM_021754	Nucleolar protein 5	Nol5
1373200_at	XM_001063564	Eukaryotic translation elongation factor 1 epsilon 1 (predicted)	Eef1e1_predicted
1388560_at	NM_001008771	WD repeat domain 77	Wdr77
1374945_at	NM_001007706	GCD14/PCMT domain containing protein RGD1359191	RGD1359191
1376737_at	XM_001073157	EST	LOC686259
1388397_at	NM_001008721	EBNA1 binding protein 2	Ebna1bp2
1371785_at	NM_181086	Tumor necrosis factor receptor superfamily, member 12a	Tnfrsf12a
1375895_at	–	EST	–
1367764_at	NM_012923	Cyclin G1	Ccng1
1388674_at	NM_080782	Cyclin-dependent kinase inhibitor 1A	Cdkn1a
1373499_at	NR_002704	Growth arrest specific 5	Gas5
1386897_at	NM_024363	Heterogeneous nuclear ribonucleoproteins methyltransferase-like 2 (*S. cerevisiae*)	Hrmt1l2
1372211_at	NM_145673	v-maf musculoaponeurotic fibrosarcoma oncogene family, protein K (avian)	Mafk
1386995_at	NM_017259	B-cell translocation gene 2, anti-proliferative	Btg2
1372510_at	NM_001047858	Sulfiredoxin 1 homolog (*S. cerevisiae*)	Srxn1
1388900_at	XM_001076548	RGD1566118 (predicted)	RGD1566118_predicted
1370583_s_at	NM_012623	ATP-binding cassette, sub-family B (MDR/TAP), member 1A/1B	Abcb1a/Abcb1b
1398756_at	NM_012992	Nucleophosmin 1	Npm1
1375224_at	NM_001012206	Pleckstrin homology-like domain, family A, member 3	Phlda3
1388155_at	NM_053976	Keratin complex 1, acidic, gene 18	Krt1-18
1368032_at	NM_022869	Nucleolar and coiled-body phosphoprotein 1	Nolc1
1388629_at	NM_199099	Inosine 5-monophosphate dehydrogenase 2	Impdh2
1371936_at	NM_199372	Eukaryotic translation initiation factor 4A1	Eif4a1
1377387_a_at	–	EST	–
1374326_at	NM_001011980	Peter pan homolog (Drosophila)	Ppan
1367617_at	NM_012495	Aldolase A	Aldoa
1376001_at	XM_001065234	Polymerase (RNA) I associated factor 1 (predicted)	Praf1_predicted
1398832_at	NM_012749	Nucleolin	Ncl
1368121_at	NM_013215	Aldo-keto reductase family 7, member A3 (aflatoxin aldehyde reductase)	Akr7a3
1370174_at	NM_133546	Myeloid differentiation primary response gene 116	Myd116
1398771_at	NM_019283	Solute carrier family 3, member 2	Slc3a2
1389450_at	XM_001071583	EST	LOC360830
1371530_at	NM_199370	Keratin complex 2, basic, gene 8	Krt2-8
1367834_at	NM_053464	Spermidine synthase	Srm
1387282_at	NM_053612	Heat shock 22 kDa protein 8	Hspb8
1372043_at	XM_001071573	EST	RGD1311709_predicted
1372150_at	NM_001034146	Ubiquitin-specific protease 10	Usp10
1389569_at	NM_001029915	Brix domain containing 2	Bxdc2
1371498_at	NM_001037348	JTV1	MGC125271
1389815_at	NM_172045	Protein phosphatase 1, regulatory (inhibitor) subunit 14B	Ppp1r14b
1370314_at	NM_031148	Solute carrier family 20, member 1	Slc20a1
1372218_at	NM_199410	WD repeat domain 12	Wdr12
1372354_at	–	EST	–
1367654_at	NM_031819	Fat tumor suppressor homolog (Drosophila)	Fath
1388107_at	NM_144746	Protein phosphatase 2, regulatory subunit B, delta isoform	Ppp2r2d
1372028_at	NM_001047095	EST	RGD1305727_predicted
1373767_at	NM_001008363	Zinc finger, AN1-type domain 2A	Zfand2a
1390579_at	XM_001073162	EST	RGD1305222_predicted
1388588_at	NM_001015013	Mammary tumor virus receptor 2	Mtvr2
1370309_a_at	NM_031330	Heterogeneous nuclear ribonucleoprotein A/B	Hnrpab
1367732_at	NM_030987	Guanine nucleotide binding protein, beta 1	Gnb1
1399158_a_at	NM_012992	Nucleophosmin 1	Npm1
1389577_at	NM_001009640	Cirrhosis, autosomal recessive 1A (human)	Cirh1a
1398757_at	NM_012992	Nucleophosmin 1	Npm1
1370947_at	XM_001070821	EST	Rda279
1373677_at	XM_001061829	Solute carrier family 39 (zinc transporter), member 10 (predicted)	Slc39a10_predicted
1388244_s_at	NM_017138	Ribosomal protein SA	Rpsa
1388150_at	NM_053490	Exportin 1, CRM1 homolog (yeast)	Xpo1
1388666_at	NM_001003401	Ectodermal-neural cortex 1	Enc1
1367713_at	NM_019356	Eukaryotic translation initiation factor 2, subunit 1 alpha	Eif2s1
1386910_a_at	NM_024148	Apurinic/apyrimidinic endonuclease 1	Apex1
1372019_at	XM_001062474	EST	RGD1310128_predicted
1373647_at	NM_001009652	Zinc finger protein 622	Zfp622
1387072_at	NM_053794	Protein kinase, lysine deficient 1	Prkwnk1
1388754_at	–	EST	–
1367870_at	NM_032614	Thioredoxin-like 2	Txnl2

Table 2 (*Continued*)

Probe ID	Accession number	Gene title	Gene symbol
1387950_at	NM_138847	Nuclear import 7 homolog (*S. cerevisiae*)	Nip7
1387807_at	NM_031763	Platelet-activating factor acetylhydrolase, isoform Ib, alpha subunit 45 kDa	Pafah1b1
1371378_at	XM_001053247	EST	LOC678808
1371735_at	–	EST	–
1398791_at	NM_031614	Thioredoxin reductase 1	Txnrd1
1386958_at	NM_031614	Thioredoxin reductase 1	Txnrd1
1385616_a_at	XM_001059946	ASF1 anti-silencing function 1 homolog A (*S. cerevisiae*) (predicted)	Asf1a_predicted
1388990_at	NM_139186	Mki67 (FHA domain) interacting nucleolar phosphoprotein	Mki67ip
1388449_at	XM_001071102	Eukaryotic translation elongation factor 1 beta 2 (predicted)	Eef1b2_predicted
1373850_at	NM_001025737	Sphingomyelin phosphodiesterase, acid-like 3B	Smpdl3b
1371539_at	XM_001071992	Nucleolar protein family A, member 2 (predicted)	Nola2_predicted
1387774_at	NM_013011	Tyrosine 3-monooxygenase/tryptophan 5-monooxygenase activation protein, zeta polypeptide	Ywhaz
1371980_at	NM_001034922	ATPase family, AAA domain containing 3A	Atad3a
1373075_at	XM_001061556	EST	RGD1560888_predicted
1367693_at	NM_013052	Tyrosine 3-monooxygenase/tryptophan 5-monooxygenase activation protein, eta polypeptide	Ywhah
1387973_at	NM_173123	Cytochrome P450, family 4, subfamily f, polypeptide 4	Cyp4f4
1390317_at	–	EST	–
1371377_at	NM_001037346	Ribosomal protein S19	Rps19
1373380_at	NM_001010963	Brain zinc finger protein	LOC362154
1367590_at	NM_053439	RAN, member RAS oncogene family	Ran
1370295_at	NM_138548	Expressed in non-metastatic cells 1	Nme1
1374632_at	NM_001012143	Phosphatidylserine receptor	Ptdsr
1388381_at	NM_001013095	Eukaryotic translation initiation factor 3, subunit 4 (delta)	Eif3s4
1370785_s_at	NM_152935	Translocase of outer mitochondrial membrane 20 homolog (yeast)	Tomm20
1398801_at	NM_134415	CDK105 protein	Cdk105
1374764_at	XM_001058941	EST	RGD1305605_predicted
1374793_at	XM_001065786	WD repeat domain 3 (predicted)	Wdr3_predicted
1368106_at	NM_031821	polo-like kinase 2 (Drosophila)	Plk2
1372116_at	XM_001079091	Mitochondrial ribosomal protein S2 (predicted)	Mrps2_predicted
1388507_at	NM_001037352	Integrin beta 4 binding protein	Itgb4bp
1389200_at	NM_182674	Bystin-like	Bysl
1372558_at	XM_001053949	NMDA receptor-regulated gene 1 (predicted)	Narg1_predicted
1371809_at	NM_212534	Mitochondrial ribosomal protein S18B	Mrps18b
1387911_at	NM_138708	RAB geranylgeranyl transferase, b subunit	Rabggtb
1372243_at	XM_001063411	Calcium binding protein 39 (predicted)	Cab39_predicted
1372255_at	XM_001065238	Arginyl-tRNA synthetase (predicted)	Rars_predicted
1370184_at	NM_017147	Cofilin 1, non-muscle	Cfl1
1372461_at	NM_001012504	EST	Set_predicted

compounds including APL, AA, and BBr (Fig. 4o–q), and remaining 16 (Fig. 4r) were correctly predicted as negative.

3.4. Additional biological validation

In order to support the class discrimination results by PAM, hepatic total glutathione was quantified for the following selected samples: high dose MP- and TAA-treated groups, and BBZ-treated groups.

Hepatic glutathione contents transiently reduced with peak values at 3H for MP, 6H for TAA and 9H for BBZ after single dosing, and rapidly recovered 24H after the treatment (Fig. 5). Although hepatic glutathione content was kept at normal or higher in the BBZ-treated group at all time points of repeated dose study, in the MP- and TAA-treated groups it reduced with repeated dosing (Fig. 5). These time course changes of the glutathione contents are clearly correlated with the change of the PAM score.

Of the PPARα agonists, only WY, but not CFB and GFZ, showed positive scores at 15D and 29D. If the PAM classifier detects carcinogenesis via the activation of PPARα and these three agonists stimulated the receptor to the same extent, all of three agonists should have been classified as positive. The dose of each compound had been determined based on a 7-day repeated preliminary study and thus the doses would not be proportional to their potency to the receptor. To assess the biological potency of each agonist *in vivo*, we compared the induction of acyl-coenzyme A oxidase 1, a gene directly regulated by PPARα. As shown in Fig. 6, the dose of WY appeared to be too high, since enzyme induction reached its maximum by the low dose of WY. During repeated administrations, however, the extent of the induction was almost the same as in the high dose of these three agonists. If the positive score of WY was due to its PPARα activation, not only the high dose but also the middle and low dose should be classified as positive. We then performed PAM using the present classifier for the three doses of these three agonists, but no positive scores were obtained other than the high dose of WY at 15D and 29D (data not shown).

4. Discussion

The goal of the present study was to develop a classifier for early assessment of potential non-genotoxic hepatocarcinogenic-

Table 3
GO analysis of the PAM classifier

Term	Count	Percentage	p-Value
Cellular metabolism	41	34.75	5.07E−03
Primary metabolism	38	32.20	1.80E−02
Macromolecule metabolism	31	26.27	8.64E−04
Cell organization and biogenesis	22	18.64	3.84E−05
Biosynthesis	14	11.86	8.19E−03
Cellular localization	12	10.17	3.03E−04
Cell proliferation	10	8.47	6.26E−03
Negative regulation of physiological process	10	8.47	1.66E−02
Negative regulation of cellular process	10	8.47	2.75E−02
Protein localization	9	7.63	7.12E−03
Cell cycle	9	7.63	1.10E−02
Cell death	8	6.78	4.27E−02
Cellular morphogenesis	7	5.93	2.60E−02
Response to DNA damage stimulus	5	4.24	2.58E−02
Regulation of response to stimulus	2	1.69	2.33E−02

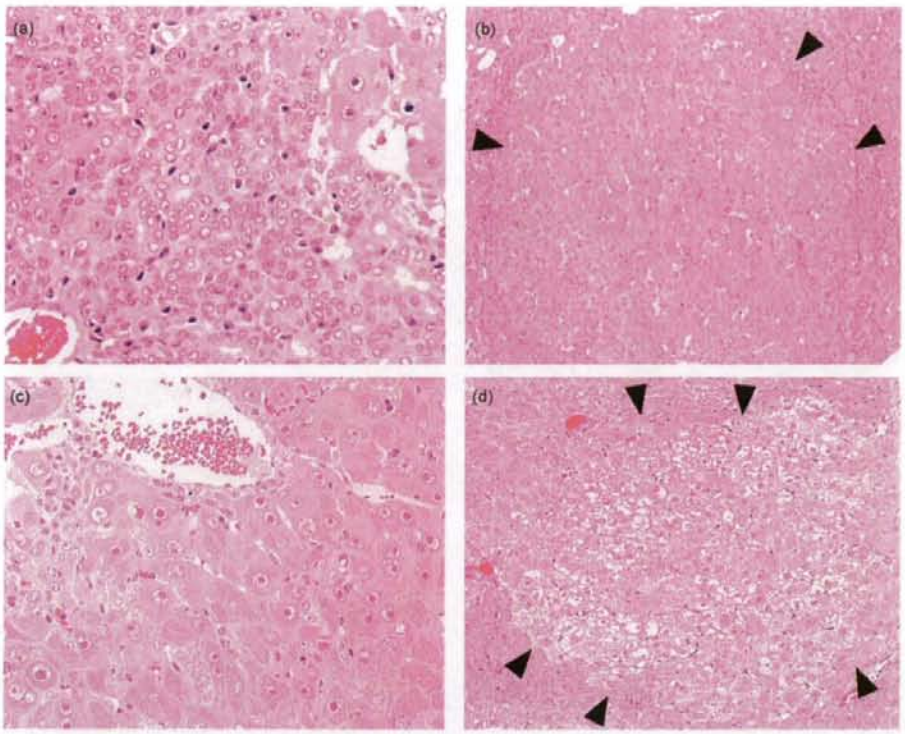

Fig. 1. Histopathology of rat liver treated with MP or TAA for 28 days. Repeated administrations of high dose of MP (100 mg/kg) for 28 days caused hepatocellular hyperplasia and some affected portal regions contained increased numbers of oval cells arranged in clusters without a distinct lumen (a), and in some cases, a pre-neoplastic altered hepatocellular focus was seen (b; arrowheads). In the centrilobular region of rat liver treated with repeated administrations of high dose of TAA (45 mg/kg) for 28 days, hepatocytes exhibited hypertrophy with large, atypical nuclei (c). As in methapyrilene, a pre-neoplastic altered hepatocellular focus was also observed (d; arrowheads).

ity of chemicals based on gene expression changes stored in our database, TG-GATEs. In order to utilize the classifier for practical drug development, we did not attempt to explore an original algorism but to use a well-established one, *i.e.*, PAM in the present case. Our advantage over the previous similar works was the quality of the database, *i.e.*, the quantitative gene expression data obtained in the single platform employing standardized and enriched protocol with three dose levels and eight time points (four for single and four for repeated). The enrichment of time and dose in the data has been shown to be quite powerful in toxicological analysis in various

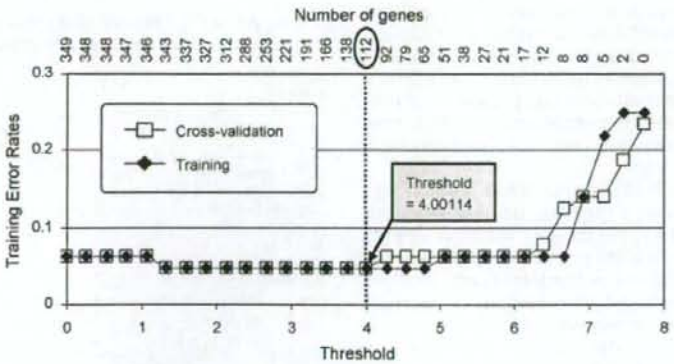

Fig. 2. PAM training and cross validation. PAM training was performed by comparing 2 positive compounds (MP and TAA, high dose group only) with 6 negative compounds (APAP, ASA, PhB, RIF, ANIT and AM) on the ratio of expression levels of the selected 349 probe sets for various time points (total of 64 training samples). Ten-fold cross validation was performed to find out the optimal classifier performance, which minimized classification errors for training sets. Both the training (black symbol) and cross-validated errors (white symbol) were minimized near the threshold = 4.00, where 112 genes (circled) were selected.

(a)

		Prediction results			
		Positive	Negative	Class Error Rate	Overall Error Rate
Training	Positive	13	3	0.19	0.05
	Negative	0	48	0.00	

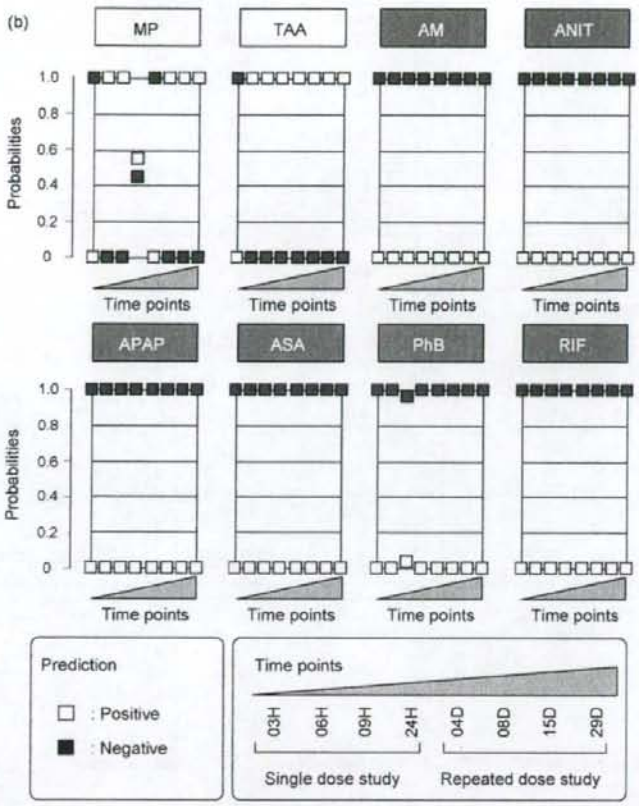

Fig. 3. Class discrimination by PAM. PAM prediction results for the condition determined in Fig. 2 are shown. (a) Prediction results of the training sets (13 positives and 48 negatives) are shown. Note that the overall success rate was 95%, *i.e.*, 13 of the 16 positive sets (81%) and all of the negative sets (100%) were correctly classified. (b) Prediction result of individual sample. For each chemical, the samples are aligned with time as shown on the bottom. The samples predicted as positive are depicted with white and negative with black. Note that two out of three errors occurred at 3 h after single dosing.

ways (Urushidani, 2007). In the present study, genes showing clear dose- and time-dependent changes were successfully extracted by K-means clustering, and we could detect the changes of the score transient after single administration which then turned to be sustained after repeated administration. These also helped us consider the toxicological mechanism.

After PAM training, we produced a discriminator consisting of 112 of the mobilized probe sets that could discriminate between both classes with a high probability, >95%. In the training procedure, MP-3H, 4D, and TAA-3H were judged as false negatives. However, these results were considered to be reasonable because 3H of both compounds was too early for development of hepatotoxicity and 4D of MP treatment was the period when homeostatic recovery of the hepatic glutathione contents occurred.

In the present experiments, MP and TAA showed similar early morphological changes in rat liver, characterized as hepatocellular single cell necrosis with inflammatory response and hypertrophy with granular eosinophilic changes. This was confirmed by electron microscopy as proliferation and swelling of mitochondria (unpublished observations). In addition, hepatocellular altered foci were observed at 15D and/or 29D in the MP and TAA-treated groups. It is well known that this type of lesion is a pre-neoplastic transformation of the cells and is induced in the early stage of non-genotoxic hepatocarcinogenesis in the liver (Bannasch, 1976; Fischer et al., 1983). Therefore, early gene expression profiling in liver treated with these two compounds is considered to be closely related to future carcinogenesis.

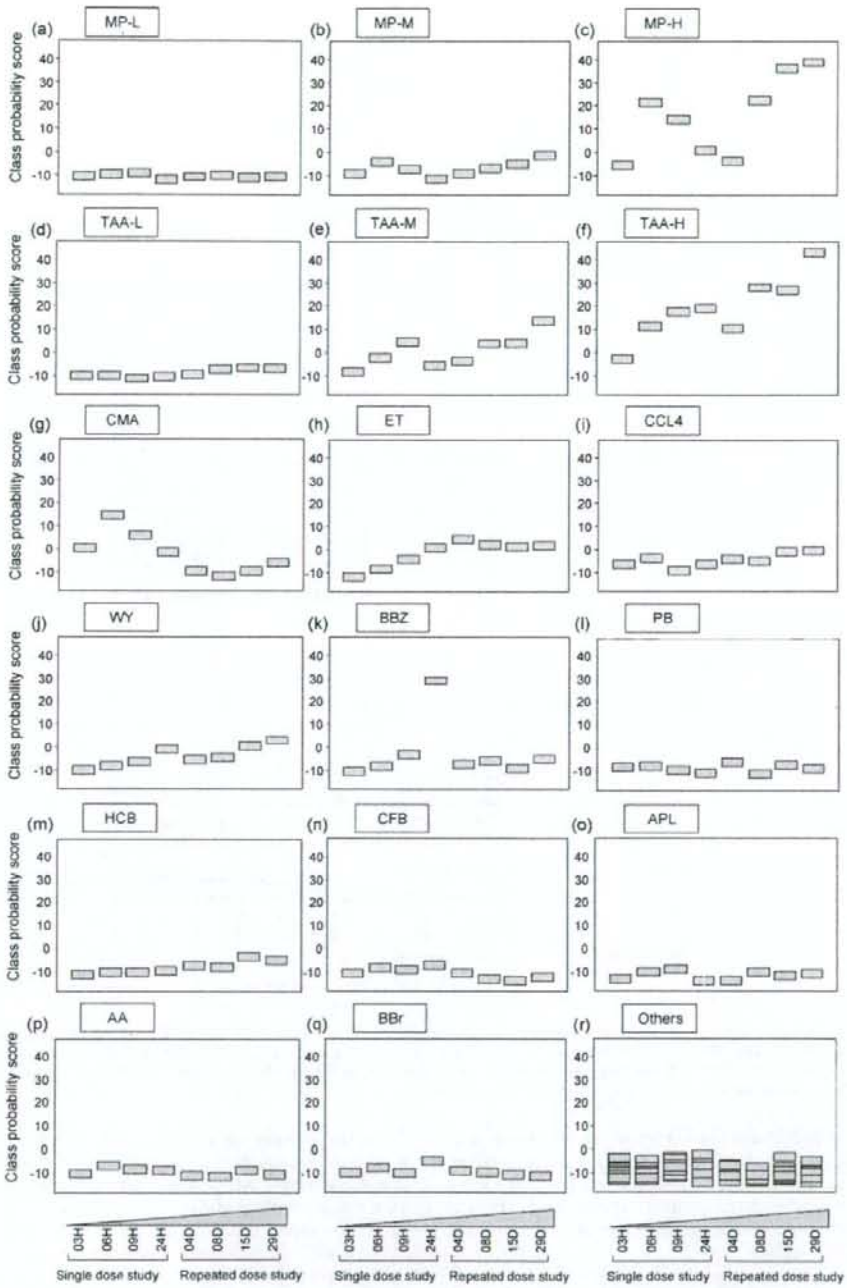

Fig. 4. PAM prediction score. The PAM class probability was converted to a score as described in Section 2 in order to enable quantitative comparison. The score is shown for MP ((a) 10 mg/kg, L; (b) 30 mg/kg, M; (c) 100 mg/kg, H), TAA ((d) 4.5 mg/kg, L; (e) 15 mg/kg, M; (f) 45 mg/kg, H), CMA ((g) 150 mg/kg), ET ((h) 250 mg/kg), CCL4 ((i) 300 mg/kg), WY ((j) 100 mg/kg), BBZ ((k) 300 mg/kg), PB ((l) 100 mg/kg), HCB ((m) 300 mg/kg), CFB ((n) 300 mg/kg), APL ((o) 150 mg/kg), AA ((p) 30 mg/kg), BBr ((q) 200 mg/kg), and (r) the other 17 chemicals. For abbreviation of the compounds, see Table 1.

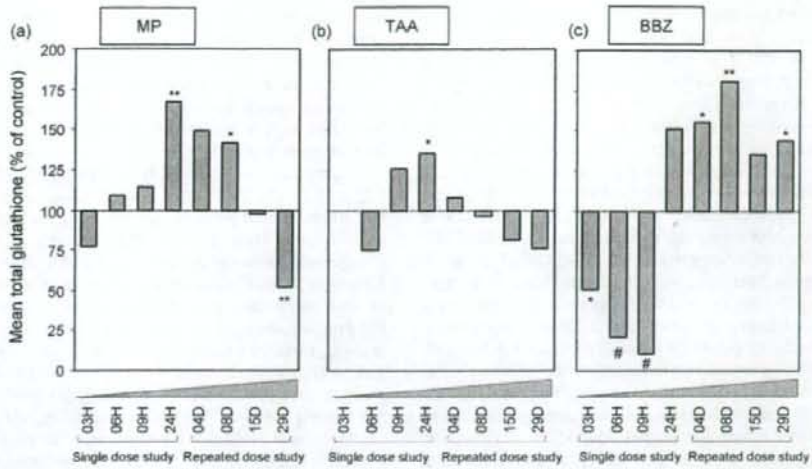

Fig. 5. Effects of MP, TAA or BBZ on glutathione contents in rat liver. Hepatic total glutathione was measured in the liver of rats receiving a high dose of MP (a), TAA (b) or BBZ (c), and their corresponding controls. Measurements were performed for five rats per group using Glutathione Quantification Kit. The results were expressed as percent of control at each time point. Statistical analysis was done by an unpaired two-tailed Student's *t*-test or Welch's *t*-test as appropriate. $^{*}p<0.05$, $^{**}p<0.01$, by Student's *t*-test, $\#p<0.05$ by Welch's *t*-test.

The gene list selected as a marker for predicting hepatic carcinogenicity contained oxidative stress-, oxidative DNA damage-, and cell cycle regulation-related genes, which were changed in the early stage of administration. The oxidative stress is due to the production of reactive oxygen species more than the anti-oxidant capability of the target cells. Unregulated or prolonged production of cellular oxidants has been thought to lead to mutation as a result of oxidant-induced DNA damage, thought to participate in non-genotoxic carcinogenesis (Klaunig et al., 1998; Klaunig and Kamendulis, 2004). The observed expression changes in these genes is in accordance with previous reports that the repetitive cycle of DNA damage (initiation) and reproduction (promotion) caused by sustained oxidative stress is closely related to the carcinogenic process of non-genotoxic carcinogens. This does not mean that the classifier detects any compounds causing oxidative stress. Of the compounds used as negative sets, APAP is known as a prototypic oxidative stressor, which induces glutathione depletion in liver when overdosed (James et al., 2003; Kiyosawa et al., 2004). ASA was reported to induce some antioxidant enzymes and components (Cai et al., 1995), and stimulates some beta-oxidation enzymes, bringing about an overproduction of H_2O_2 (Rivero et al., 1994). PhB was reported to accelerate glutathione oxidation and it induces lipid peroxidation of microsomes (Miura et al., 2002). All of these were successfully classified as negative, suggesting that the classifier discriminates non-carcinogens causing oxidative stress.

The validity of the presently developed discriminator for carcinogenesis was examined on our large-scale database, and all of the 20 chemicals except BBZ (selected as a non-carcinogen) were judged as negative at any time points. Of the eight chemicals classified as non-genotoxic carcinogens, CMA, ET, CCl4 and WY showed positive prediction and increase in the PAM prediction scores in repeated administrations, whereas enzyme inducers such as PB and HCB, and other peroxisome proliferators were all judged as negative.

For CMA (Lake et al., 2002; National Toxicol Program, 1993), ET (Ogiso et al., 1990; Svardal et al., 1988), and CCl4 (Castro et al., 1989; Natarajan et al., 2006), oxidative stress was reported as being involved in their hepatotoxicity and carcinogenesis. It could be con-

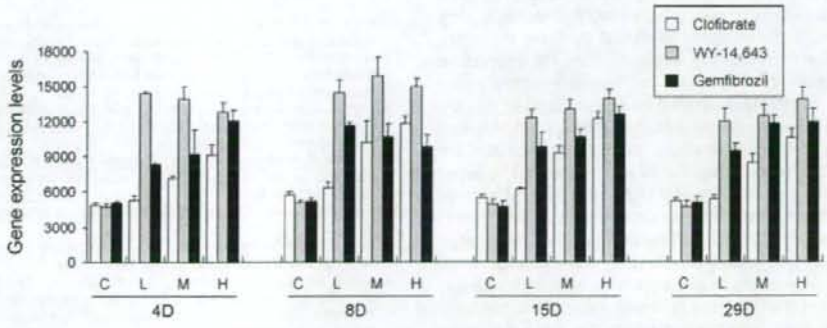

Fig. 6. Effects of repeated administration of CFB, WY or GFZ on expression of acyl-CoA oxidase-1. Expression of acyl-CoA oxidase-1, a gene directly regulated by PPARα, was measured by GeneChip, and the intensities were normalized for each chip by setting the mean intensity to 500 (per chip normalization). The results were expressed as mean ± S.D. ($n=3$). For each panel, C: control, L: low dose, M: middle dose, H: high dose, for CFB: 30, 100, 300 mg/kg; WY: 10, 30, 100 mg/kg; GFZ: 30, 100, 300 mg/kg, respectively.

cluded that sustained oxidative stress plays an important role in their carcinogenesis, as in MP and TAA.

The induction of PPARα in rodents treated with peroxisome proliferators was considered to be related to hepatocarcinogenesis (Holden and Tugwood, 1999). Moreover, increased levels of H_2O_2 generation, hydroxyl free-radical formation and lipid peroxidation were found in the liver of rats following long-term treatment with peroxisome proliferators. It was also reported that 8-hydroxydeoxyguanosine was found in the liver DNA of rats chronically treated with a PPARα (Reddy and Lalwai, 1983; Reddy and Rao, 1989). In the present study, our discriminator designated WY as positive among the PPARα agonists, CFB, GFZ, and WY. This result suggests that either the discriminator could predict the carcinogenesis of PPARα agonists (although its sensitivity is relatively low) or that WY had an additional carcinogenicity differing from other PPARα agonists. The latter would be more likely since the low and middle doses of WY (by which the induction of acyl-CoA oxidase 1 reached a maximum) did not classify as positive and since the highest doses of CFB and GFZ induce acyl-CoA oxidase 1 to almost the same extent as WY. It was also suggested that WY might share a carcinogenic mechanism with MP and TAA apart from its PPARα agonist's activity.

The P450 enzymes generate oxygen free radicals in the process of metabolizing xenobiotic chemicals (Parke and Ioannides, 1990), including PB (Utley and Mehendale, 1991) and HCB (Smith and De Matteis, 1990). Kinoshita et al. (2002) reported that PB-induced reversible alteration to nuclear 8-hydroxydeoxyguanosine by oxidative stress in rat liver after several days of continuous application. Furthermore, Elrick et al. (2005) provided evidence for the relationship between oxidative stress and PB-induced non-genotoxic hepatic carcinogenesis. On the other hand, HCB exposure induces long-term alterations in intercellular communication via gap junction in rat liver. This effect is thought to be a critical mechanism of HCB-induced non-genotoxic hepatocarcinogenesis and tumor promotion (Plante et al., 2002). However, these chemicals were classified as non-carcinogens based on gene expression profiling. There are likely to be numerous mechanisms involved in non-genotoxic rodent hepatic carcinogenesis. Therefore, it is thought that these chemicals induce non-genotoxic hepatocarcinogenesis through chemical-specific mechanisms.

For the evaluation of these results of prediction, we developed a PAM prediction score based on the positive/negative class probability. In the present study, we compared the score with the hepatic glutathione contents in order to examine the validity of the prediction. In association with the largest decrease of hepatic glutathione contents at 3H (MP), 6H (TAA) and 9H (BBZ), the PAM prediction score increased with the peak at 6H (MP), 9H (TAA) and 24H (BBZ). This could be explained as follows: hepatic glutathione was rapidly consumed to detoxify the oxidants produced by these toxicants, and in the subsequent glutathione-depleted state the expression of these marker genes was up-regulated. The excess production of glutathione for homeostasis tended to decrease in MP or TAA, whereas its high value was maintained in BBZ during their repeated administrations. It is known that some reactive intermediates are conjugated with glutathione to be excreted from the cell. The hepatotoxicity of the acute dose of BBZ was significantly reduced by prior sub-chronic exposure to BBZ. Therefore, the enhanced BBZ excretion by glutathione conjugation could partly explain such potential tolerance against its acute hepatotoxicity (Chakrabarti and Brodeur, 1984). It would be reasonable to speculate that BBZ, which causes transient hepatic and DNA damage by oxidative stress at the early stage of dosing, does not result in hepatic cancer since metabolic protection against oxidative stress does not allow the sustained stressful condition up to 28 days of administration, whereas a breakdown of protection occurs in the case of MP and TAA suggested by the glutathione contents. There was a close correlation between the pattern of change in glutathione and PAM scores, supporting the usefulness of the present marker genes. The present scoring system also enables us to make a prediction based on important toxicological points, *e.g.*, dose- and time-dependency and it would be a quite convenient way for evaluation of the results of discriminant analysis.

In summary, we showed that the expression profile of 112 genes selected by the PAM method could make a prediction of oxidative stress-related hepatocarcinogenicity with high precision at the early stage of administration. The possibility of non-genotoxic carcinogenicity is suggested as early as 24 h after the single dosing. Although pseudo-positives are included in the chemicals selected by the single dose experiments, these can be discriminated by the prediction based on repeated administration up to 28 days. At present, tests for carcinogenicity using rats takes at least 2 years. The present study has suggested a possibility to enable it to take as short as 28 days with high precision. Although neither a single gene nor a single pathway is sufficient to predict non-genotoxic hepatocarcinogens at present, it is evident that combinations of biomarker gene sets appeared to be useful for prediction of carcinogenesis. Further study is clearly necessary to clarify the pathophysiological roles of the genes included in the marker gene list for the process of carcinogenesis.

Conflict of interest

None.

Acknowledgement

This study was supported by a grant from the Ministry of Health, Labour and Welfare of Japan (H14-toxico-001).

Appendix A. Supplementary data

Supplementary data associated with this article can be found, in the online version, at doi:10.1016/j.tox.2008.05.013.

References

Agoston, M., Orsi, F., Feher, E., Hagymasi, K., Orosz, Z., Blazovics, A., Feher, J., Vereckei, A., 2003. Silymarin and vitamin E reduce amiodarone-induced lysosomal phospholipidosis in rats. Toxicology 190, 231–241.

Bannasch, P., 1976. Cytology and cytogenesis of neoplastic (hyperplastic) hepatic nodules. Cancer Res. 36, 2555–2562.

Becker, F.F., 1983. Thioacetamide hepatocarcinogenesis. J. Natl. Cancer Inst. 71, 553–558.

Butterworth, B.E., Bogdanffy, M.S., 1999. A comprehensive approach for integration of toxicity and cancer risk assessments. Regul. Toxicol. Pharmacol. 29, 23–36.

Cai, Y., Appelkvist, E.L., DePierre, J.W., 1995. Hepatic oxidative stress and related defenses during treatment of mice with acetylsalicylic acid and other peroxisome proliferators. J. Biochem. Toxicol. 10, 87–94.

Castro, G.D., Diaz Gomez, M.I., Castro, J.A., 1989. Species differences in the interaction between CCl4 reactive metabolites and liver DNA or nuclear protein fractions. Carcinogenesis 10, 289–294.

Chakrabarti, S., Brodeur, J., 1984. Dose-dependent metabolic excretion of bromobenzene and its possible relationship to hepatotoxicity in rats. J. Toxicol. Environ. Health. 14, 379–391.

Cohen, S.M., Ellwein, L.B., 1990. Cell proliferation in carcinogenesis. Science 249, 1007–1011.

Combes, R.D., 2000. The use of structure-activity relationships and markers of cell toxicity to detect non-genotoxic carcinogens. Toxicol. In Vitro 14, 387–399.

Delaney, J., Neville, W.A., Swain, A., Miles, A., Leonard, M.S., Waterfield, C.J., 2004. Phenylacetylglycine, a putative biomarker of phospholipidosis: its origins and relevance to phospholipid accumulation using amiodarone treated rats as a model. Biomarkers 9, 271–290.

Diez-Fernandez, C., Sanz, N., Alvarez, A.M., Zaragoza, A., Cascales, M., 1998. Influence of aminoguanidine on parameters of liver injury and regeneration induced in rats by a necrogenic dose of thioacetamide. Br. J. Pharmacol. 125, 102–108.

Dragan, Y.P., Sargent, L., Xu, Y.D., Xu, Y.H., Pitot, H.C., 1993. The initiation-promotion-progression model of rat hepatocarcinogenesis. Proc. Soc. Exp. Biol. Med. 202, 16–24.

Duivenvoorden, W.C., Maier, P., 1994. Nongenotoxic carcinogens shift cultured rat hepatocytes into G1 cell cycle phase: influence of tissue oxygen tension on cells with different ploidy. Eur. J. Cell. Biol. 64, 368–375.

Ellinger-Ziegelbauer, H., Gmuender, H., Bandenburg, A., Ahr, H.J., 2008. Prediction of a carcinogenic potential of rat hepatocarcinogens using toxicogenomics analysis of short-term in vivo studies. Mutat. Res. 637, 23–39.

Ellinger-Ziegelbauer, H., Stuart, B., Wahle, B., Bomann, W., Ahr, H.J., 2005. Comparison of the expression profiles induced by genotoxic and nongenotoxic carcinogens in rat liver. Mutat. Res. 575, 61–84.

Elrick, M.M., Kramer, J.A., Alden, C.L., Blomme, E.A., Bunch, R.T., Cabonce, M.A., Curtiss, S.W., Kier, L.D., Kolaja, K.L., Rodi, C.P., Morris, D.L., 2005. Differential display in rat livers treated for 13 weeks with phenobarbital implicates a role for metabolic and oxidative stress in nongenotoxic carcinogenicity. Toxicol. Pathol. 33, 118–126.

Fielden, M.R., Brennan, R., Gollub, J., 2007. A gene expression biomarker provides early prediction and mechanistic assessment of hepatic tumor induction by nongenotoxic chemicals. Toxicol. Sci. 99, 90–100.

Fischer, G., Altmannsberger, M., Schauer, A., Katz, N., 1983. Early stages of chemically induced liver carcinogenesis by oral administration of the antihistaminic methapyrilene hydrochloride. J. Cancer Res. Clin. Oncol. 106, 53–57.

Giri, A.K., 1993. The genetic toxicology of paracetamol and aspirin: a review. Mutat. Res. 296, 199–210.

Hayashi, Y., 1992. Overview of genotoxic carcinogens and non-genotoxic carcinogens. Exp. Toxicol. Pathol. 44, 465–471.

Holden, P.R., Tugwood, J.D., 1999. Peroxisome proliferator-activated receptor alpha: role in rodent liver cancer and species differences. J. Mol. Endocrinol. 22, 1–8.

Iida, M., Anna, C.H., Holliday, W.M., Collins, J.B., Cunningham, M.L., Sills, R.C., Devereux, T.R., 2005. Unique patterns of gene expression changes in liver after treatment of mice for 2 weeks with different known carcinogens and non-carcinogens. Carcinogenesis 26, 689–699.

James, L.P., Mayeux, P.R., Hinson, J.A., 2003. Acetaminophen-induced hepatotoxicity. Drug Metab. Dispos. 31, 1499–1506.

Jean, P.A., Roth, R.A., 1995. Naphthylisothiocyanate disposition in bile and its relationship to liver glutathione and toxicity. Biochem. Pharmacol. 50, 1469–1474.

Kinoshita, A., Wanibuchi, H., Imaoka, S., Ogawa, M., Masuda, C., Morimura, K., Funae, Y., Fukushima, S., 2002. Formation of 8-hydroxydeoxyguanosine and cell-cycle arrest in the rat liver via generation of oxidative stress by phenobarbital: association with expression profiles of p21(WAF1/Cip1), cyclin D1 and Ogg1. Carcinogenesis 23, 341–349.

Kiyosawa, N., Ito, K., Sakuma, K., Niino, N., Kanbori, M., Yamoto, T., Manabe, S., Matsunuma, N., 2004. Evaluation of glutathione deficiency in rat livers by microarray analysis. Biochem. Pharmacol. 68, 1465–1475.

Klaunig, J.E., Kamendulis, L.M., 2004. The role of oxidative stress in carcinogenesis. Annu. Rev. Pharmacol. Toxicol. 44, 239–267.

Klaunig, J.E., Xu, Y., Isenberg, J.S., Bachowski, S., Kolaja, K.L., Jiang, J., Stevenson, D.E., Walborg Jr., E.F., 1998. The role of oxidative stress in chemical carcinogenesis. Environ. Health Perspect. 106, 289–295.

Lake, B.G., Evans, J.G., Chapuis, F., Walters, D.G., Price, R.J., 2002. Studies on the disposition, metabolism and hepatotoxicity of coumarin in the rat and Syrian hamster. Food. Chem. Toxicol. 40, 809–823.

Leonard, T.B., Popp, J.A., Graichen, M.E., Dent, J.G., 1981. alpha-Naphthylisothiocyanate induced alterations in hepatic drug metabolizing enzymes and liver morphology: implications concerning anticarcinogenesis. Carcinogenesis 2, 473–482.

Lijinsky, W., Reuber, M.D., Blackwell, B.N., 1980. Liver tumors induced in rats by oral administration of the antihistaminic methapyrilene hydrochloride. Science 209, 817–819.

Meakawa, A., Onodera, H., Tanigawa, H., Furuta, K., Kanno, J., Matsuoka, C., Ogiu, T., Hayashi, Y., 1987. Long-term studies on carcinogenicity and promoting effect of phenylbutazone in DONRYU rats. J. Natl. Cancer. Inst. 79, 577–584.

Melnick, R.L., Kohn, M.C., Portier, C.J., 1996. Implications for risk assessment of suggested nongenotoxic mechanisms of chemical carcinogenesis. Environ. Health Perspect. 104, 123–134.

Miller, E.C., Miller, J.A., 1981. Mechanisms of chemical carcinogenesis. Cancer 47, 1055–1064.

Miura, T., Muraoka, S., Fujimoto, Y., 2002. Lipid peroxidation induced by phenylbutazone radicals. Life Sci. 70, 2611–2621.

Natarajan, S.K., Thomas, S., Ramamoorthy, P., Basivireddy, J., Pulimood, A.B., Ramachandran, A., Balasubramanian, K.A., 2006. Oxidative stress in the development of liver cirrhosis: a comparison of two different experimental models. J. Gastroenterol. Hepatol. 21, 947–957.

National Toxicol Program, 1993. NTP toxicology and carcinogenesis studies of coumarin (CAS No. 91-64-5) in F344/N rats and B6C3F1 mice (gavage studies). Natl. Toxicol. Progr. Tech. Rep. Ser. 422, 1–340.

National Toxicology Program, 1990. NTP toxicology and carcinogenesis studies of phenylbutazone (CAS No. 50-33-9) in F344/N rats and B6C3F1 mice (gavage studies). Natl. Toxicol. Progr. Tech. Rep. Ser. 367, 1–205.

National Toxicology Program, 1993. Toxicology and carcinogenesis studies of acetaminophen (CAS No. 103-90-2) in F344 rats and B6C3F1 mice (feed studies). Natl. Toxicol. Progr. Tech. Rep. Ser. 394, 1–274.

National Toxicology Program, 2000. NTP hepatotoxicity studies of the liver carcinogen methapyrilene hydrochloride (CAS No. 135-23-9) administered in feed to male F344/N rats. Toxic. Rep. Ser. 46, 1–C7.

Nie, A.Y., McMillian, M., Parker, J.B., Leone, A., Bryant, S., Yieh, L., Bittner, A., Nelson, J., Carmen, A., Wan, J., Lord, P.G., 2006. Predictive toxicogenomics approaches reveal underlying molecular mechanisms of nongenotoxic carcinogenicity. Mol. Carcinogen. 45, 914–933.

Nguyen-Ba, G., Vasseur, P., 1999. Epigenetic events during the process of cell transformation induced by carcinogens. Oncol. Rep. 6, 925–932.

Ogiso, T., Tatematsu, M., Tamano, S., Hasegawa, R., Ito, N., 1990. Correlation between medium-term liver bioassay system data and results of long-term testing in rats. Carcinogenesis 11, 561–566.

Ohshima, M., Ward, J.M., Brennan, L.M., Creasia DA, 1984. A sequential study of methapyrilene hydrochloride-induced liver carcinogenesis in male F344 rats. J. Natl. Cancer Inst. 72, 759–768.

Ohtsuka, M., Fukuda, K., Yano, H., Kojiro, M., 1998. Immunohistochemical measurement of cell proliferation as replicative DNA synthesis in the liver of male Fischer 344 rats following a single exposure to nongenotoxic hepatocarcinogens and noncarcinogens. Exp. Toxicol. Pathol. 50, 13–17.

Parke, D.V., Ioannides, C., 1990. Role of cytochromes P-450 in mouse liver tumor production. Prog. Clin. Biol. Res. 331, 215–230.

Plante, I., Charbonneau, M., Cyr, D.G., 2002. Decreased gap junctional intercellular communication in hexachlorobenzene-induced gender-specific hepatic tumor formation in the rat. Carcinogenesis 23, 1243–1249.

Ratra, G.S., Morgan, W.A., Mullervy, J., Powell, C.J., Wright, M.C., 1998. Methapyrilene hepatotoxicity is associated with oxidative stress, mitochondrial disfunction and is prevented by the Ca^{2+} channel blocker verapamil. Toxicology 130, 79–93.

Reddy, J.K., Lalwai, N.D., 1983. Carcinogenesis by hepatic peroxisome proliferators: evaluation of the risk of hypolipidemic drugs and industrial plasticizers to humans. Crit. Rev. Toxicol. 12, 1–58.

Reddy, J.K., Rao, M.S., 1989. Oxidative DNA damage caused by persistent peroxisome proliferation: its role in hepatocarcinogenesis. Mutat. Res. 214, 63–68.

Rivero, A., Monreal, J.I., Gil, M.J., 1994. Peroxisome enzyme modification and oxidative stress in rat by hypolipidemic and antiinflammatory drugs. Rev. Esp. Fisiol. 50, 259–268.

Sanz, N., Diez-Fernandez, C., Fernandez-Simon, L., Alvarez, A., Cascales, M., 1995. Relationship between antioxidant systems, intracellular thiols and DNA ploidy in liver of rats during experimental cirrhogenesis. Carcinogenesis 16, 1585–1593.

Scott, R.E., Wille Jr., J.J., Wier, M.L., 1984. Mechanisms for the initiation and promotion of carcinogenesis: a review and a new concept. Mayo Clin. Proc. 59, 107–117.

Silva Lima, B., Van der Laan, J.W., 2000. Mechanisms of nongenotoxic carcinogenesis and assessment of the human hazard. Regul. Toxicol. Pharmacol. 32, 135–143.

Smith, A.G., De Matteis, F., 1990. Oxidative injury mediated by the hepatic cytochrome P-450 system in conjunction with cellular iron. Effects on the pathway of haem biosynthesis. Xenobiotica 20, 865–877.

Sodhi, C.P., Rana, S., Mehta, S., Vaiphei, K., Goel, R.C., Mehta, S.K., 1997. Study of oxidative-stress in rifampicin-induced hepatic injury in growing rats with and without protein-energy malnutrition. Hum. Exp. Toxicol. 16, 315–321.

Svardal, A.M., Ueland, P.M., Aarsaether, N., Aarsland, A., Berge, R.K., 1988. Differential metabolic response of rat liver, kidney and spleen to ethionine exposure. S-adenosylamino acids, homocysteine and reduced glutathione in tissues. Carcinogenesis 9, 227–232.

Takashima, K., Mizukawa, Y., Morishita, K., Okuyama, M., Kasahara, T., Toritsuka, N., Miyagishima, T., Nagao, T., Urushidani, T., 2006. Effect of the difference in vehicles on gene expression in the rat liver-analysis of the control data in the Toxicogenomics Project Database. Life Sci. 78, 2787–2796.

Tibshirani, R., Hastie, T., Narasimhan, B., Chu, G., 2002. Diagnosis of multiple cancer types by shrunken centroids of gene expression. Proc. Natl. Acad. Sci. U.S.A. 99, 6567–6572.

Uehara, T., Kiyosawa, N., Hirode, M., Omura, K., Shimizu, T., Ono, A., Mizukawa, Y., Miyagishima, M., Nagao, T., Urushidani, T., 2008a. Gene expression profiling of methapyrilene-induced hepatotoxicity in rat. J. Toxicol. Sci. 33, 37–50.

Uehara, T., Kiyosawa, N., Shimizu, T., Omura, K., Hirode, M., Imazawa, T., Mizukawa, Y., Ono, A., Mizukawa, Y., Miyagishima, M., Nagao, T., Urushidani, T., 2008b. Species differences in coumarin-induced hepatotoxicity as an example of how toxicogenomics help assessing risks for human. Human Exp. Toxicol. 27, 23–35.

Urushidani, T., 2007. Prediction of hepatotoxicity based on the toxicogenomics database. In: Sahu, S.C. (Ed.), Hepatotoxicity from Genomics to In Vitro and In Vivo Models. Wiley & Sons, pp. 507–529.

Utley, W.S., Mehendale, H.M., 1991. Evidence for stimulated glutathione synthesis by phenobarbital pretreatment during an oxidative challenge in isolated hepatocytes. J. Biochem. Toxicol. 6, 101–113.

Weisburger, J.H., Williams, G.M., 2000. The distinction between genotoxic and epigenetic carcinogens and implication for cancer risk. Toxicol. Sci. 57, 4–5.

Williams, G.M., Iatropoulos, M.J., Weisburger, J.H., 1996. Chemical carcinogen mechanisms of action and implications for testing methodology. Exp. Toxicol. Pathol. 48, 101–111.

Available online at www.sciencedirect.com
ScienceDirect
Toxicology and Applied Pharmacology 229 (2008) 290–299
Toxicology and Applied Pharmacology
www.elsevier.com/locate/ytaap

Gene expression profiling in rat liver treated with compounds inducing phospholipidosis

Mitsuhiro Hirode [a,b], Atsushi Ono [b,c], Toshikazu Miyagishima [b], Taku Nagao [d], Yasuo Ohno [c], Tetsuro Urushidani [b,e,*]

[a] Development Research Center, Pharmaceutical Research Division, Takeda Pharmaceutical Company Limited, Yodogawa-ku, Osaka, 532-8686, Japan
[b] Toxicogenomics Project, National Institute of Biomedical Innovation, Ibaraki, Osaka, 567-0085, Japan
[c] National Institute of Health Sciences, Setagaya-ku, Tokyo 158-8501, Japan
[d] Food Safety Commission of Japan, Chiyoda-ku, Tokyo, 100-8989, Japan
[e] Department of Pathophysiology, Doshisha Women's College of Liberal Arts, Kyotanabe, Kyoto 610-0395, Japan

Received 27 October 2007; revised 14 January 2008; accepted 19 January 2008
Available online 14 February 2008

Abstract

We have constructed a large-scale transcriptome database of rat liver treated with various drugs. In an effort to identify a biomarker for diagnosis of hepatic phospholipidosis, we extracted 78 probe sets of rat hepatic genes from data of 5 drugs, amiodarone, amitriptyline, clomipramine, imipramine, and ketoconazole, which actually induced this phenotype. Principal component analysis (PCA) using these probes clearly separated dose- and time-dependent clusters of treated groups from their controls. Moreover, 6 drugs (chloramphenicol, chlorpromazine, gentamicin, perhexiline, promethazine, and tamoxifen), which were reported to cause phospholipidosis but judged as negative by histopathological examination, were designated as positive by PCA using these probe sets. Eight drugs (carbon tetrachloride, coumarin, tetracycline, metformin, hydroxyzine, diltiazem, 2-bromoethylamine, and ethionamide), which showed phospholipidosis-like vacuolar formation in the histopathology, could be distinguished from the typical drugs causing phospholipidosis. Moreover, the possible induction of phospholipidosis was predictable by the expression of these genes 24 h after single administration in some of the drugs. We conclude that these identified 78 probe sets could be useful for diagnosis of phospholipidosis, and that toxicogenomics would be a promising approach for prediction of this type of toxicity.

Keywords: Phospholipidosis; Toxicogenomics; Rat; Liver; Principal component analysis

Introduction

The toxicogenomics project was a 5-year collaborative project by the National Institute of Biomedical Innovation (NIBIO), the National Institute of Health Science (NIHS), and 15 pharmaceutical companies in Japan that started in 2002 (Urushidani and Nagao, 2005). Its aim was to construct a large-scale toxicology database of transcriptome for prediction of toxicity of new chemical entities in the early stage of drug development. About 150 chemicals, mainly medicinal compounds, were selected, and gene expression in liver (also kidney in some cases) was comprehensively analyzed by using Affymetrix GeneChip®. In 2007, the project was finished and the whole system, consisting of the database, the analyzing system and the prediction system, was completed and named as TG-GATEs (Genomics Assisted Toxicity Evaluation System developed by the Toxicogenomics Project, Japan). The present mission is to identify potential biomarker gene lists useful for prediction or diagnosis of drug-induced hepato- and nephro-toxicity using this system.

In toxicity studies, phospholipidosis (PLsis) is often observed in various tissues including liver, kidney, and lung. PLsis is a lipid storage disease characterized by intracellular accumulation of phospholipids and the appearance of membranous lamellar inclusions known as lamellar bodies. Its pathogenesis has been thought to be the unbalance of phospholipid turnover. As for drug-induced PLsis, it is well known that cationic

* Corresponding author. Department of Pathophysiology, Doshisha Women's College of Liberal Arts, Kyotanabe, Kyoto 610-0395, Japan. Fax: +81 774 65 8689.
E-mail address: turushid@dwc.doshisha.ac.jp (T. Urushidani).

0041-008X/$ - see front matter © 2008 Elsevier Inc. All rights reserved.
doi:10.1016/j.taap.2008.01.036

amphiphilic drugs (CADs), characterized by a hydrophobic ring structure and a hydrophilic side chain with a charged amine group have the potential to cause PLsis. Therefore, it has been postulated that drug-induced PLsis involves direct binding of CADs to phospholipids, subsequently creating a complex that is resistant to degradation by phospholipases (Reasor et al., 2006). There is also an observation that some CADs can cause PLsis by directly inhibiting phospholipase activity (Halliwell, 1997; Reasor et al., 2006). Although much effort has been done to establish the methods to predict PLsis of drugs (Tomizawa et al., 2006), sensitive diagnostic markers and effective prognostic markers are still desired.

In the present study, we selected PLsis in liver as a target phenotype, and tried to identify candidate biomarkers that enable the cell to discriminate chemicals with the potential to cause this phenotype for application of TG-GATEs.

Materials and methods

Compounds. Compounds used for the data analysis are listed in Table 1, in which the chemical name, abbreviation, dosage, administration route and vehicle used in the study are summarized.

Animal treatment. The experiments were carried out as previously described in the literature (Takashima et al., 2006). Male Crl:CD(SD) rats were purchased from Charles River Japan Inc., (Kanagawa, Japan) at 5-weeks of age. After a 7-day quarantine and acclimatization period, the animals were divided into groups of 5 animals using a computerized stratified random grouping method based on body weight for each age. The animals were individually housed in stainless-steel cages in a room that was lighted for 12 h (7:00–19:00) daily, ventilated with an air-exchange rate of 15 times per hour, and maintained at 21–25 °C with a relative humidity of 40–70%. Each animal was allowed free access to water and pellet food (CRF-1, sterilized by radiation, Oriental Yeast Co., Japan). Rats in each group were orally administered with various drugs suspended or dissolved either in 0.5% methylcellulose solution (MC) or corn oil according to their dispersibility, except for gentamicin and 2-bromoethylamine, which were dissolved in saline and administered intravenously. The animals were treated for 3, 7, 14 or 28 days and sacrificed 24 h after the last dosing. Blood samples were collected to a heparinized tube under ether anesthesia from the abdominal aorta after which the animals were euthanized.

The experimental protocols were reviewed and approved by the Ethics Review Committee for Animal Experimentation of the National Institute of Health Sciences.

Microarray analysis. After collecting the blood, the animals were euthanized by exsanguination from the abdominal aorta under ether anesthesia. An aliquot of the sample (about 30 mg) for RNA analysis was obtained from the left lateral lobe of the liver in each animal immediately after termination, kept in RNAlater® (Ambion, Austin, TX, USA) overnight at 4 °C, and then frozen at −80 °C until use. Liver samples were homogenized with the buffer RLT supplied in RNeasy Mini Kit (Qiagen, Valencia, CA, USA), and total RNA was isolated according to the manufacturer's instructions. Microarray analysis was conducted on 3 out of 5 samples for each group by using GeneChip® Rat Genome 230 2.0 Arrays (Affymetrix, Santa Clara, CA, USA), containing 31,042 probe sets. The procedure was conducted basically according to the manufacturer's instructions using Superscript Choice System (Invitrogen, Carlsbad, CA, USA) and T7-(dT)24-oligonucleotide primer (Affymetrix) for cDNA synthesis, cDNA Cleanup Module (Affymetrix) for purification, and BioArray High yield RNA Transcript Labeling Kit (Enzo Diagnostics, Farmingdale, NY, USA) for synthesis of biotin-labeled cRNA. Ten micrograms of fragmented cRNA was hybridized to a Rat Genome 230 2.0 Array for 18 h at 45 °C at 60 rpm, after which the array was washed and stained by streptavidin–phycoerythrin using Fluidics Station 400 (Affymetrix) and scanned by Gene Array Scanner (Affymetrix). The digital image files were processed by Affymetrix Microarray Suite version 5.0. Microarray image data were analyzed with GeneChip Operating Software (Affymetrix).

The digital image files were processed by Affymetrix Microarray Suite version 5.0 and the intensities were normalized for each chip by setting the mean intensity to 500 (per chip normalization).

Statistical analysis. In order to extract probe sets related to PLsis, we first employed gene expression data of rat liver treated with repeated administration for 3, 7, 14, and 28 days of AM, AMT, CPM, IMI and KC in our database, and they are known to cause PLsis, and in fact, the induction of this disease was confirmed in the present study.

After removing the probe sets with Affymetrix absent call in the whole 48 sample set ($N=3$ for 4 time points and 4 dose levels for one drug), differentially

Table 1
Compounds

Compound name	Abbreviation	Dose (dose level, mg/kg)			Administration route	Vehicle
		Low	Middle	High		
Amiodarone	AM	200/20*	600/60*	2000/200*	PO	MC
Amitriptyline	AMT	15	50	150	PO	MC
Clomipramine	CPM	10	30	100	PO	MC
Imipramine	IMI	10	30	100	PO	MC
Ketoconazole	KC	10	30	100	PO	MC
Chloramphenicol	CMP	100	300	1000	PO	MC
Chlorpromazine	CPZ	4.5	45/15*	150/45*	PO	MC
Gentamicin	GMC	10	30	100	IV	SA
Perhexiline	PH	15	50	150	PO	MC
Promethazine	PMZ	20	60	200	PO	MC
Tamoxifen	TMX	6	20	60	PO	CO
Carbon tetrachloride	CCl4	30	100	300	PO	CO
Coumarin	CMA	15	50	150	PO	CO
Tetracycline	TC	100	300	1000	PO	MC
Metformin	MFM	100	300	1000	PO	MC
Hydroxyzine	HYZ	10	30	100	PO	MC
Diltiazem	DIL	80	240	800	PO	MC
2-bromoethylamine	BEA	6/2*	20/6*	60/20*	IV	SA
Ethionamide	ETH	100/30*	300/100*	1000/300*	PO	MC

*: as single dose/repeated dose.
PO: peroral, IV: intravenous.
MC: 0.5 w/v% methylcellulose; SA: saline; CO: corn oil.

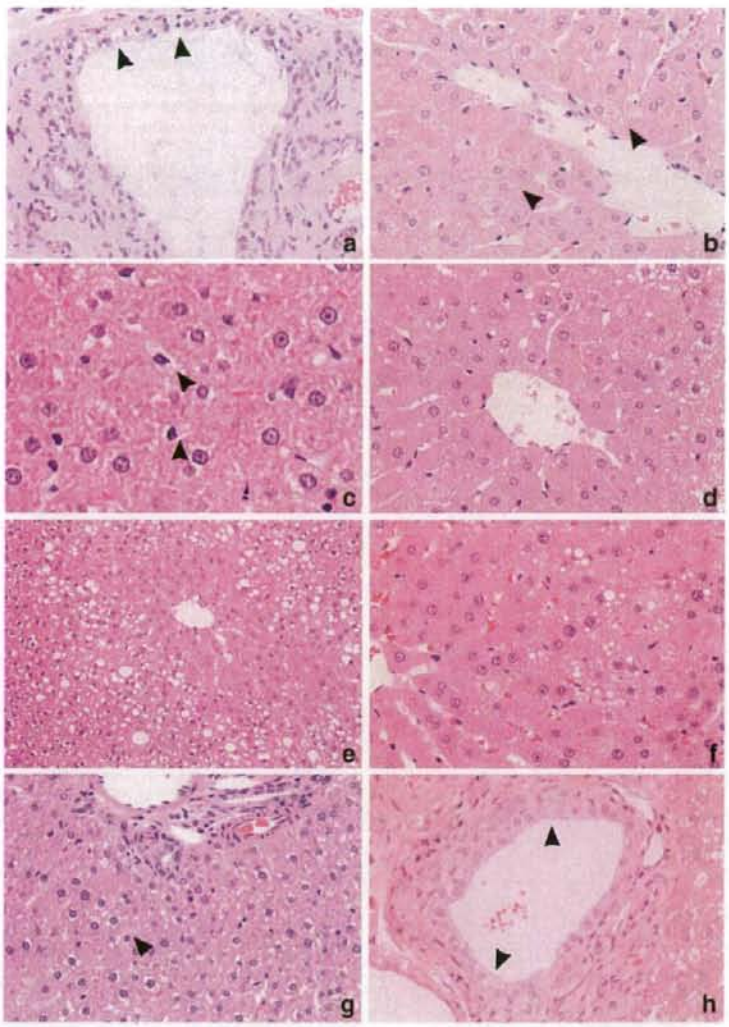

Fig. 1. Histopathology of rat liver treated with amiodarone, amitriptyline, clomipramine, imipramine, and ketoconazole. a–c. Amiodarone 200 mg/kg, 29th day. Vacuolations in the bile duct cell (a) in the hepatocyte (b) and in the Kupffer cell (c) are evident (arrowheads). d. Amitriptyline 150 mg/kg, 29th day. Vacuolation in the hepatocyte is evident. e. Clomipramine 100 mg/kg, 29th day. Vacuolation is noted in the midlobular hepatocytes. f–g. Imipramine 100 mg/kg, 29th day. Vacuolations in the hepatocyte (f) and in the Kupffer cell (g) are evident. h. Ketoconazole 100 mg/kg, 29th day. Vacuolation occurs exclusively in the bile duct (arrowheads).

expressed genes by the treatment were extracted by Welch's ANOVA ($p<0.05$) for the dose level at any time point. This procedure was continued for 4 time points and genes showing significant change, and any points were combined as PLsis responsive genes. In the next step, commonly mobilized genes among these 5 chemicals were selected.

Principal component analysis (PCA) of the GeneChip data was also performed using Spotfire DecisionSite.

Pathway and gene ontology (GO) analysis. The identified probe sets were subjected to analysis of Kyoto Encyclopedia of Genes and Genomes (KEGG) pathway and GO analysis by DAVID (Database for Annotation, Visualization, and Integrated Discovery; http://apps1.niaid.nih.gov/david/ using Fisher's exact test (Dennis et al., 2003). Level 5 analysis was adopted.

Results

Histopathological examination

The results of histopathological examination of 5 compounds (AM, AMT, CPM, IMI and KC) known to induce PLsis are shown in Fig. 1 and Table 2. For most cases, clear vacuolization was observed in the cytoplasm of hepatocytes, and this change tended to progress with dose and time. Vacuolation was also noted in Kupffer cell (AM, IMI) or bile duct (AM). In the case of KC, vacuolation occurred exclusively in the bile duct.

Table 2
Histopathological findings

Compound	Findings	Time	Dose		
			Low	Middle	High
AM	Vacuolization, bile duct cell	3 h–4 day	–	–	–
		8 day	–	–	3/5(±)
		15 day	–	–	1/5(±), 4/5(+)
		29 day	–	–	4/4(+)
	Vacuolization, hepatocyte	3 h–8 day	–	–	–
		15 day	–	–	2/5(±)
		29 day	–	–	4/4(±)
	Vacuolization, Kupffer cell	3 h–8 day	–	–	–
		15 day	–	–	5/5(±)
		29 day	–	–	4/4(±)
AMT	Vacuolization, hepatocyte	3 h–4 day	–	–	–
		8 day	–	–	4/5(±)
		15 day	–	1/5(±)	5/5(+)
		29 day	–	1/5(±), 2/5(+)	1/3(+), 2/3(2+)
CPM	Vacuolization, hepatocyte	3 h–15 day	–	–	–
		29 day	–	–	1/5(±), 1/5(+)
IMI	Vacuolization, hepatocyte	3 h–4 day	–	–	–
		8 day	–	–	4/5(±)
		15 day	–	–	1/5(±), 2/5(+)
		29 day	–	2/5(±)	1/4(±), 3/4(+)
	Vacuolization, Kupffer cell	3 h–8 day	–	–	–
		15 day	–	–	3/5(±)
		29 day	–	–	–
KC	Vacuolization, bile duct cell	3 h–24 h	–	–	–
		4 day	–	–	5/5(+)
		8 day	–	–	5/5(+)
		15 day	–	1/5(+)	2/5(+), 3/5(2+)
		29 day	–	1/5(±), 4/5(+)	5/5(2+)
CMP	Abnormality	3 h–29 day	–	–	–
CPZ	Abnormality	3 h–29 day	–	–	–
GMC	Abnormality	3 h–29 day	–	–	–
PH	Abnormality	3 h–29 day	–	–	–
PMZ	Abnormality	3 h–29 day	–	–	–
TMX	Abnormality	3 h–29 day	–	–	–
CCl4	Degeneration, fatty, hepatocyte	3 h–9 h	–	–	–
		24 h	–	2/5(±)	1/5(±), 4/5(+)
		4 day	4/5(±), 1/5(+)	5/5(+)	1/5(±), 4/5(+)
		8 day	1/5(±), 4/5(+)	5/5(+)	4/5(+), 1/5(2+)
		15 day	1/5(±), 4/5(+)	5/5(+)	4/5(+), 1/5(2+)
		29 day	5/5(+)	4/5(+), 1/5(2+)	2/5(+), 2/5(2+), 1/5(3+)
CMA	Vacuolization, hepatocyte	3 h–8 day	–	–	–
		15 day	–	–	2/5(±), 1/5(+)
		29 day	–	–	5/5(+)
TC	Vacuolization, hepatocyte	3 h–8 day	–	–	–
		15 day	–	–	2/5(±)
		29 day	–	–	2/5(±)
MFM	Deposit, glycogen, hepatocyte	3 h–24 h	–	–	–
		4 day	–	2/5(±)	5/5(±)
		8 day	–	–	2/5(±)
		15 day	–	–	2/5(±)
		29 day	–	–	1/5(±)
HYZ	Vacuolization, hepatocyte	3 h–8 day	–	–	–
		15 day	–	–	2/5(±), 2/5(+)
		29 day	–	–	4/5(+), 1/5(2+)
DIL	Vacuolization, hepatocyte	3 h–4 day	–	–	–
		8 day	–	–	2/5(±)
		15 day	–	1/5(±)	5/5(±)
		29 day	–	4/5(±)	4/4(±)
BEA	Vacuolization, hepatocyte	3 h–8 day	–	–	–
		15 day	–	–	2/5(+)
		29 day	–	4/5(+)	4/5(+)
ETH	Vacuolization, hepatocyte	3 h–24 h	–	–	–
		4 day	–	4/5(+), 1/5(2+)	5/5(+)
		8 day	–	3/5(±), 2/5(+)	3/3(+)
		15 day	–	2/5(±), 3/5(+)	2/5(±), 3/5(+)
		29 day	–	2/5(+)	NA

–: not remarkable, ±: minimal, +: mild, 2+: moderate, 3+: severe, NA: not applicable.

Microarray data analysis

Differentially expressed genes with statistical significance were extracted from each of 5 representative drugs inducing PLsis, as described in the Materials and methods section. The numbers of extracted probe sets were 4915 for AM, 3565 for AMT, 1907 for CPM, 2339 for IMI, and 3482 for KC. We then selected the probe sets that were commonly changed in all compounds and 78 probe sets were obtained. The list of these probe sets is shown in Table 3. Based on gene ontology, the contents of genes related to carboxylic acid metabolism, electron transport, amino acid metabolism, amine catabolism, and nitrogen compound catabolism were significantly high (Table 4). Although not significant, 4 lipid biosynthesis-related genes were contained. This feature might reflect the cellular changes related to lipid metabolism in association with PLsis.

Principal component analysis (PCA)

Using the 78 probe sets extracted as above, PCA was performed on the 5 drugs inducing PLsis. As shown in Fig. 2,

Table 3
List of 78 probe sets changed in 5 compounds inducing PLsis

Probe set ID	Gene title	Gene symbol
1367676_at	High mobility group box 2	Hmgb2
1367819_at	Glutamate oxaloacetate transaminase 2, mitochondrial	Got2
1368016_at	Peroxisomal *trans*-2-enoyl-CoA reductase	Pecr
1368171_at	Lysyl oxidase	Lox
1368213_at	P450 (cytochrome) oxidoreductase	Por
1368275_at	Sterol-C4-methyl oxidase-like	Sc4mol
1368403_at	Retinoblastoma-like 2	Rbl2
1368467_at	Cytochrome P450, family 4, subfamily F, polypeptide 2	Cyp4f2
1368520_at	Apolipoprotein A-IV	Apoa4
1368618_at	Growth factor receptor bound protein 14	Grb14
1368718_at	Aldehyde dehydrogenase family 1, subfamily A4	Aldh1a4
1368778_at	Solute carrier family 6 (neurotransmitter transporter, taurine), member 6	Slc6a6
1368905_at	Carboxylesterase 2 (intestine, liver)	Ces2
1368931_at	SH3-domain GRB2-like 3	Sh3gl3
1368977_a_at	Fractured callus expressed transcript 1	Fxc1
1369275_s_at	Cytochrome P450 IIA1 (hepatic steroid hydroxylase IIA1) gene	Cyp2a1
1369737_at	cAMP responsive element modulator	Crem
1369850_at	UDP-glucuronosyltransferase 2 family, polypeptide A1	Ugt2a1
1370004_at	H2A histone family, member Y	H2afy
1370054_at	Cyclin-dependent kinase inhibitor 2C (p18, inhibits CDK4)	Cdkn2c
1370375_at	Glutaminase 2 (liver, mitochondrial)	Gls2
1370583_s_at	ATP-binding cassette, subfamily B (MDR/TAP), member 1	Abcb1
1370613_s_at	UDP glycosyltransferase 1 family, polypeptide A1	Ugt1a1
1370698_at	Liver UDP-glucuronosyltransferase, phenobarbital-inducible form liver	Udpgtr2
1371076_at	Cytochrome P450, family 2, subfamily b, polypeptide 15	Cyp2b15
1371089_at	Transcribed locus	–
1371412_a_at	Neuronal regeneration related protein	Nrep
1371546_at	Similar to TR4 orphan receptor-associated protein TRA16	LOC361128
1371680_at	Similar to gamma-aminobutyric acid (GABA(A)) receptor-associated protein-like 1	LOC683917
1371809_at	Mitochondrial ribosomal protein S18B	Mrps18b
1371875_at	Mannosidase, beta A, lysosomal	Manba
1372056_at	CKLF-like MARVEL transmembrane domain containing 6	Cmtm6
1372124_at	Eukaryotic translation initiation factor 4B	Eif4b
1372181_at	Similar to expressed sequence AA408877	RGD1308513
1372479_at	Transcribed locus, moderately similar to NP_064456.1 fibrinogen, beta polypeptide [*Rattus norvegicus*]	–
1372602_at	Similar to genethonin 1	RGD1311800
1372885_at	Transcribed locus	–
1373015_at	Ring finger protein 11 (predicted)	Rnf11_predicted
1373626_at	Transcribed locus	–
1373823_at	Similar to cyclin-dependent kinases regulatory subunit 2 (CKS-2) (predicted)	RGD1562047_predicted
1373924_at	Similar to C530044N13Rik protein	RGD1306568
1373970_at	Similar to RIKEN cDNA 9230117N10	RGD1311155
1374531_at	Transcribed locus	–
1374953_at	Similar to CG12279-PA	LOC500420
1375423_at	MAX-like protein X	Mlx
1375637_at	Similar to RIKEN cDNA 1110003E01	RGD1311122
1375909_at	Similar to glutathione transferase GSTM7-7	MGC108896
1377019_at	Transcribed locus	–
1378016_at	Echinoderm microtubule associated protein-like 4 (predicted)	Eml4_predicted
1380254_at	Transcribed locus, moderately similar to NP_079928.1 general transcription factor III A [*Mus musculus*]	–
1384169_a_at	Vav2 oncogene (predicted)	Vav2_predicted
1386857_at	Stathmin 1	Stmn1
1386917_at	Pyruvate carboxylase	Pc
1387006_at	Rat senescence marker protein 2A gene, exons 1 and 2	Smp2a
1387022_at	Aldehyde dehydrogenase family 1, member A1	Aldh1a1
1387031_at	Endoplasmic reticulum protein 29	Erp29
1387093_at	Solute carrier organic anion transporter family, member 1a4	Slco1a4
1387094_at	Solute carrier organic anion transporter family, member 1a4	Slco1a4
1387109_at	P450 (cytochrome) oxidoreductase	Por
1387118_at	Cytochrome P450, family 3, subfamily a, polypeptide 1	Cyp3a1
1387203_at	Glucokinase regulatory protein	Gckr
1387223_at	Aminoadipate aminotransferase	Aadat

Table 3 (*continued*)

Probe set ID	Gene title	Gene symbol
1387307_at	Histidine ammonia lyase	Hal
1387511_at	Cytochrome P450 IIA1 (hepatic steroid hydroxylase IIA1) gene	Cyp2a1
1387665_at	Betaine-homocysteine methyltransferase	Bhmt
1387669_a_at	Epoxide hydrolase 1, microsomal	Ephx1
1387759_s_at	UDP glycosyltransferase 1 family, polypeptide A1	Ugt1a1
1387793_at	Transcribed locus, strongly similar to NP_075738.1 yippee-like 1 [*Mus musculus*]	–
1388212_a_at	RT1 class Ib, locus S3	RT1-S3
1388348_at	Transcribed locus	–
1388425_at	Similar to RIKEN cDNA D130038B21	RGD1305890
1388874_at	Metastasis suppressor 1 (predicted)	Mtss1_predicted
1389319_at	Similar to endoplasmic reticulum-Golgi intermediate compartment protein 1 (ER-Golgi intermediate compartment 32 kDa protein) (ERGIC-32)	LOC287177
1389557_at	Testis expressed gene 261	Tex261
1389986_at	CDNA clone IMAGE:7321089	–
1390455_at	Abhydrolase domain containing 2 (predicted)	Abhd2_predicted
1398754_at	Ubiquitin A-52 residue ribosomal protein fusion product 1	Uba52
1398848_at	Suppression of tumorigenicity 13	St13

treated samples were dose-dependently separated to form clusters from controls, mainly toward the direction of PC1 (contribution rate: 34.8%). In order to examine the time-dependency, all the samples were aligned on a one dimensional graph of PC1 (Fig. 3). It appears that the PC1 value generally increased with time as well as with a dose of these drugs. In case of KC, time- and dose-dependency were obscure, although the treated group clearly formed a cluster separated from the control cluster. Of the genes contributing to PC1, those with high eigenvector value were listed in Table 5. We noticed that the top 4 genes are cytochrome oxidoreductase, sterol-C4-methy oxidase-like, aldehyde dehydrogenase 1A4, and carboxylesterase 2, which are all involved in lipid metabolism.

Distinction of 6 compounds reported to induce PLsis with no abnormality in present histopathological examination

In a survey of the literature, in addition to the 5 drugs above, 6 more drugs, i.e., CMP, CPZ, GMC, PH, PMZ, and TMX in our database, are reported to induce PLsis, but no such histopathological abnormalities were confirmed in the present examination. We then applied PCA using the 78 probe sets on these 6 drugs and we show the results in Fig. 4 as a one dimensional graph with PC1. It was revealed that these 6 drugs were also separated from control clusters the same way as the 5 typical drugs inducing PLsis. Of these, some drugs such as CPZ, GMC and PH, did not change their position very much, but their extent was roughly equivalent to that of KC.

Table 4
GO analysis of identified 78 probe sets

Term	Count	Percent	*P*-value
Carboxylic acid metabolism	10	11.5	1.90E–04
Electron transport	6	6.9	1.20E–02
Amino acid metabolism	5	5.7	1.80E–02
Amine catabolism	3	3.4	3.20E–02
Nitrogen compound catabolism	3	3.4	3.40E–02
Lipid biosynthesis	4	4.6	6.10E–02

Distinction of 8 compounds showing pathological changes similar to PLsis

When examination by light microscope of HE-stained specimens is performed, we sometimes encounter a phenotype (not PLsis but another pathological change), such as lipidosis, deposition of glycogen, or hydropic degeneration, and they are quite difficult to distinguish from each other. In our database, we identified 8 drugs (CCL4, CMA, TC, MFM, HYZ, DIL, BEA, and ETH) showing such pathological changes in liver. The histopathological description of each was as follows: CCL4: "degeneration, fatty, hepatocyte"; CMA, TC, HYZ, DIL, BEA, ETH: "vacuolization, hepatocyte"; and MFM: "deposit, glycogen, hepatocyte". To examine the efficiency of the 78 probe sets, PCA was applied to these 8 pseudo-positive compounds.

As shown in Fig. 5, most of the treated samples stayed in the position close to that of the control samples. Exceptionally, HYZ and DIL formed separate clusters from the controls, as 5 standard compounds inducing PLsis.

Possible distinction of the samples 24 h after a one time dosage

The above results clearly suggested that the list of extracted 78 probe sets was a useful diagnostic marker for PLsis in rat liver. The next question is whether the list works as a prognostic marker for PLsis. To examine this possibility, we performed PCA using the list for the gene expression profile 24 h after the single dose, and practically no pathological changes had occurred at that time. As shown in Fig. 6 left, AM 20, 60, and 200 mg/kg had a high PC1 value in repeated administration for 3 days or more, whereas that in the single dose group was close to the cluster of the control group. Then we additionally performed single dose experiments using higher doses, i.e., 200,

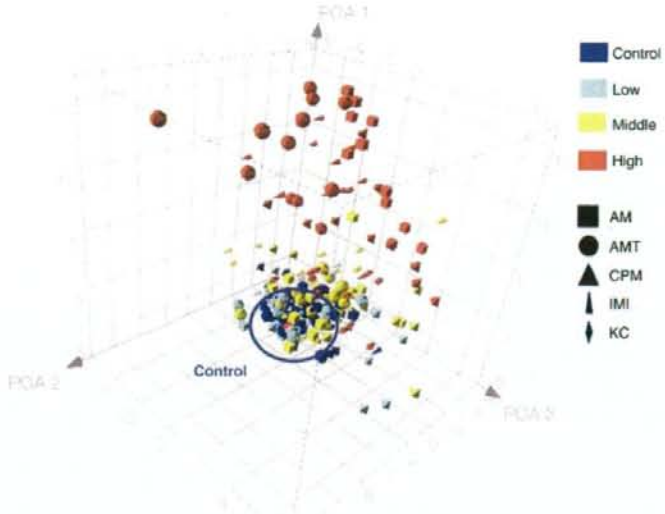

Fig. 2. Principal component analysis of gene expression profiles of amiodarone (AM), amitriptyline (AMT), clomipramine (CPM), imipramine (IMI), and ketoconazole (KC) that induced phospholipidosis in liver in the present study using the commonly mobilized 78 probe sets. Results are expressed as a three dimensional figure with PC1, 2, and 3. Treated samples were dose-dependently separated from the cluster of controls (circled by a blue line), mainly toward the direction of PC1 (contribution rate: 34.8%). For simplicity, rats receiving the same dose with different durations (3, 7, 14 and 28 days, N=3 for each; 12 total) were expressed by the same symbol.

600, and 2000 mg/kg of AM (Fig. 6, right). It was revealed that the group receiving a single dose of 2000 mg/kg AM clustered at a position clearly higher than controls with equivalent PCA1 values receiving a repeated dose of 200 mg/kg for 3 days. In the case of CPZ, the samples at 24 h after the 45 mg/kg single dosing were clearly separated from control samples to an extent more than that of the repeated dose samples (Fig. 7). We then performed additional single dose experiments using 45 and 150 mg/kg CPZ. It was clear from Fig. 7 that 150 mg/kg CPZ showed a higher PC1 value than the 45 mg/kg group.

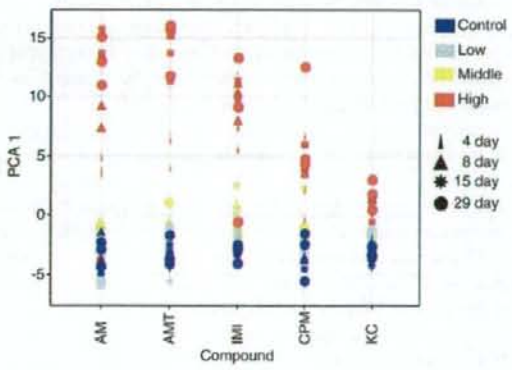

Fig. 3. Principal component analysis the same as Fig. 2 but with one dimensional expression using principal component 1. For each drug, each individual rat is depicted by a symbol with a different color and shape as shown on the right panel.

Discussion

PLsis has been one of the main concerns in the course of drug development, since its appropriate biomarkers are lacking, especially in the clinical field. In order to assess PLsis, a variety of in vitro methodologies have recently been described, e.g., using fluorescent dyes (Casartelli et al., 2003) or fluorescently labeled phospholipids (Kasahara et al., 2006, Nioi et al., 2007) in cell culture. However, these assay systems only work to estimate the potential of PLsis, but not to tell its mechanism and thus they do not help in deciding whether to go ahead or to switch to other candidates in the development process. One promising strategy would be a toxicogenomics approach. Sawada et al. (2005) recently identified a panel of 17 genes where the expression profile would predict the possibility of PLsis using HepG2 cells. This result was further transferred to a 96-well plate to attain a high throughput genomics-based platform (Sawada et al., 2006). Although the advantage of the genomics-based strategy was postulated to elucidate the background toxicological mechanism, the gene expression changes have not been related to the pathophysiological aspects of PLsis. It has been suggested that PLsis is induced by the disturbance of lipid turnover, i.e., excess of lipid biosynthesis, inhibition of lipid degradation enzymes (especially lysosomal phospholipase A2), and inhibition of lipid transporter in lysosomes. In the case of drug-induced PLsis, most of it has been attributed to the inhibition of phospholipase

Table 5
List of 28 probe sets contributing PC1

Ranking	Probe set ID	Gene title	Eigenvalue
1	1368905_at	Carboxylesterase 2 (intestine, liver)	0.165043
2	1387759_s_at	UDP glycosyltransferase 1 family, polypeptide A1	0.163056
3	1387022_at	Aldehyde dehydrogenase family 1, member A1	0.158847
4	1371076_at	Cytochrome P450, family 2, subfamily b, polypeptide 15	0.156238
5	1387118_at	Cytochrome P450, family 3, subfamily a, polypeptide 1	0.153634
6	1387109_at	P450 (cytochrome) oxidoreductase	0.152900
7	1371089_at	Transcribed locus	0.152322
8	1368718_at	Aldehyde dehydrogenase family 1, subfamily A4	0.147161
9	1370613_s_at	UDP glycosyltransferase 1 family, polypeptide A1	0.145621
10	1368977_a_at	Fractured callus expressed transcript 1	0.145613
11	1370583_s_at	ATP-binding cassette, subfamily B (MDR/TAP), member 1	0.145395
12	1380254_at	Transcribed locus, moderately similar to NP_079928.1 general transcription factor III A [*Mus musculus*]	0.145244
13	1387669_a_at	Epoxide hydrolase 1, microsomal	0.144549
14	1370698_at	Liver UDP-glucuronosyltransferase, phenobarbital-inducible form liver	0.143250
15	1368213_at	P450 (cytochrome) oxidoreductase	0.142376
16	1375423_at	MAX-like protein X	0.135972
17	1387094_at	Solute carrier organic anion transporter family, member 1a4	0.131073
18	1372602_at	Similar to genethonin 1	0.129514
19	1369850_at	UDP-glucuronosyltransferase 2 family, polypeptide A1	0.129217
20	1368275_at	Sterol-C4-methyl oxidase-like	0.129122
21	1371875_at	Mannosidase, beta A, lysosomal	0.128496
22	1372479_at	Transcribed locus, moderately similar to NP_064456.1 fibrinogen, beta polypeptide [*Rattus norvegicus*]	0.127711
23	1387093_at	Solute carrier organic anion transporter family, member 1a4	0.127266
24	1371809_at	Mitochondrial ribosomal protein S18B	0.126952
25	1384169_a_at	Vav2 oncogene (predicted)	0.125901
26	1375909_at	Similar to glutathione transferase GSTM7-7	0.125538
27	1373924_at	Similar to C530044N13Rik protein	0.122349
28	1371680_at	Similar to gamma-aminobutyric acid (GABA(A)) receptor-associated protein-like 1	0.117093

activity either through the generation of CAD-phospholipid complexes or by direct inhibition of phospholipase activity (Reasor et al., 2006). It is clearly necessary to elucidate how these changes are reflected in gene expression in order to make a prediction based on the genomics approach.

In the present study, we extracted 78 genes commonly mobilized in the 5 typical PLsis-inducing drugs, i.e., AM (Honegger et al., 1993), AMT (Drenckhahn et al., 1976), CPM (Xia et al., 2000), IMI (Drew et al., 1981; Hansson et al., 1997) and KC (Whitehouse et al., 1994). By PCA, we used these genes to successfully separate the high risk group from the low risk ones, except for KC, which showed relatively obscure separation. This is reasonable, as the histopathology of KC only causes changes

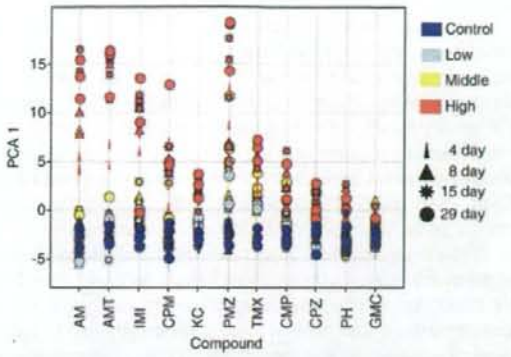

Fig. 4. Principal component analysis of gene expression profiles of 6 compounds reported to induce PLsis but no abnormality in present histopathological examination, i.e., chloramphenicol (CMP), chlorpromazine (CPZ), gentamicin (GMC), perhexiline (PH), promethazine (PMZ), and tamoxifen (TMX) using the commonly mobilized 78 probe sets. For comparison, 5 compounds shown in Figs. 2 and 3, amiodarone (AM), amitriptyline (AMT), clomipramine (CPM), imipramine (IMI), and ketoconazole (KC), are also included. Results are expressed as a one dimensional figure with PC1 (contribution rate: 34.8%). For each drug, each individual rat is depicted by a symbol with a different color and shape as shown on the right panel.

in the bile duct cells, in contrast to the other 4 drugs that elicit changes in the hepatocytes.

CMP (Joshi et al., 1989), CPZ (Kodavanti et al., 1990), GMC (Kacew, 1987), PH (Pessayre et al., 1979), PMZ (Joshi et al., 1989) and TMX (Reasor and Kacew, 2001) have also been reported to induce PLsis, but we could not detect PLsis in liver by histopathological examinations in the present study. This is not surprising when the sensitivity of detection by histopathology is

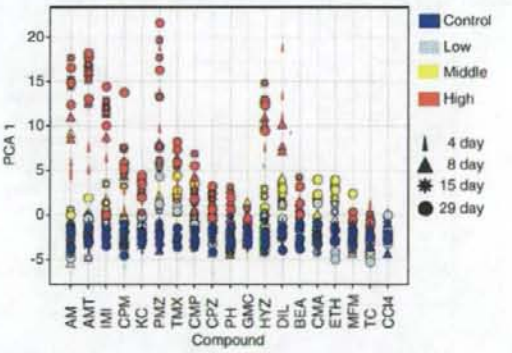

Fig. 5. Principal component analysis of gene expression profiles of 8 compounds showing pathological changes similar to PLsis, i.e., carbon tetrachloride (CCL4), coumarin (CMA), tetracycline (TC), metformin (MFM), hydroxyzine (HYZ), diltiazem (DIL), 2-bromoethylamine (BEA), and ethionamide (ETH), using the commonly mobilized 78 probe sets. For comparison, the 5 compounds shown in Figs. 2 and 3, amiodarone (AM), amitriptyline (AMT), clomipramine (CPM), imipramine (IMI) and ketoconazole (KC), and the 6 compounds in Fig. 4, chloramphenicol (CMP), chlorpromazine (CPZ), gentamicin (GMC), perhexiline (PH), promethazine (PMZ), and tamoxifen (TMX) are also included. Results are expressed as a one dimensional figure with PC1 (contribution rate: 34.8%). For each drug, each individual rat is depicted by a symbol with a different color and shape as shown on the right panel.